

# Ferromagnetism in the $SU(N)$ Kondo lattice model – $SU(N)$ double exchange and supersymmetry

Keisuke Totsuka<sup>1</sup>

<sup>1</sup>*Center for Gravitational Physics and Quantum Information,  
Yukawa Institute for Theoretical Physics, Kyoto University, Kyoto 606-8502, Japan*  
(Dated: March 21, 2023)

We study the ground-state properties of the  $SU(N)$ -generalization of the Kondo-lattice model in one dimension when the Kondo coupling  $J_K$  (both ferromagnetic and antiferromagnetic) is sufficiently strong. Both cases can be realized using alkaline-earth-metal-like cold gases in optical lattices. Specifically, we first carry out the strong-coupling expansion and identify two insulating phases (one of which is the  $SU(N)$ -analog of the well-known gapped Kondo singlet phase). We then rigorously establish that the ground state in the low-density (for  $J_K < 0$ ) or the high-density (for  $J_K > 0$ ) region is ferromagnetic. The results are accounted for by generalizing the double-exchange mechanism to  $SU(N)$  “spins”. Possible realizations of Bose-Fermi supersymmetry  $SU(N|1)$  in the (generalized)  $SU(N)$  Kondo-lattice model are discussed as well.

## I. INTRODUCTION

In physics, high symmetries have been playing crucial roles in a unified understanding of seemingly different phenomena. In such situations, we often work with simple unifying theories based on high symmetries and try to understand the actual phases by taking into account the deviation from the idealized high symmetries. In condensed-matter physics, systems with high  $SU(N)$ -symmetry ( $N \geq 3$ ) have been studied for a few decades and a variety of intriguing properties have been predicted so far. However, in the standard solid-state settings, the realization of  $SU(N)$  symmetry exploits, on top of the spin- $SU(2)$ , additional symmetries [e.g.,  $SU(2)$ -symmetry associated with orbital, valley, multiple layers, etc.] that necessitate some sort of fine-tuning or idealization [1, 2]. So far, it has not been so clear to what extent physics found in those idealized systems with perfect  $SU(N)$  symmetry is robust against possible deviations in realistic systems. The situation changed when the possibility of realizing systems with almost perfect  $SU(N)$ -symmetry using alkaline-earth(-like) cold gases has been recognized [3, 4]. This has paved the way for testing a variety of remarkable predictions made in  $SU(N)$  fermion and spin systems [5, 6] in clean and well-controlled settings. For instance, the  $SU(N)$  Mott insulator has been realized experimentally [7, 8], in which antiferromagnetic correlation among the localized  $SU(N)$  magnetic moments has been observed [9, 10]. These are the first steps toward the quantum simulation of even more exotic states of matter, e.g.,  $SU(N)$  quantum spin liquids [11–13].

The  $SU(N)$ -symmetric cold gases also provide us with a playground for multi-component itinerant fermions that are predicted to exhibit a variety of interesting phenomena such as the color superfluidity [14, 15], the “baryonic” multiple-fermion bound states (dubbed trion when  $N = 3$ ) [16–18], the generalized  $\eta$ -pairing [19], and itinerant ferromagnetism [3, 20–24]. One of the merits of using the alkaline-earth-metal fermions is that one can easily implement two additional “orbital” degrees of freedom [associated with the two  $SU(N)$ -symmetric atomic states  $g$  and  $e$ ] that enable us to simulate Kondo physics. Since the suggestion of exploring the heavy-fermion physics with the two-orbital alkaline-earth-metal fermions [4], some advances have been made

both theoretically [25–27] and experimentally [28, 29]. Although most cold-atom literature focuses on the Kondo or heavy-fermion physics in which the local moments tend to be screened by the itinerant fermions, there is yet another important state of matter, itinerant ferromagnetism, in the Kondo lattice model. In fact, in the usual ( $N = 2$ ) Kondo lattice model, it is known that the so-called double-exchange mechanism [30–32], which has been originally introduced in the context of the manganites, stabilizes ferromagnetism when the Kondo coupling is ferromagnetically large [33–35], and even when it is anti-ferromagnetic, metallic ferromagnetism is favored for sufficiently large Kondo coupling [36–39] (see, e.g., Refs. [40, 41] for reviews of the one-dimensional Kondo-lattice model).

In this paper, we will rigorously show that, even for  $N \geq 3$ , ferromagnetism is one of the dominant phases in the one-dimensional  $SU(N)$  Kondo lattice model. Some rigorous results have been obtained so far on the  $SU(N)$  itinerant ferromagnetism [20, 22–24]. What we will establish here occurs in a relatively simple setting and for a wide range of fermion densities, and only needs relatively loose conditions. The  $SU(N)$  Kondo-lattice(-type) systems not only exhibit ferromagnetic and other interesting phases but also provide us with a natural playground for emergent Bose-Fermi supersymmetry. We will try to demonstrate how supersymmetry is implemented into the low-energy degrees of freedom of the Kondo-lattice model.

This paper is structured as follows. In Sec. II, we introduce the  $SU(N)$  Kondo lattice model as a particular limit of the two-orbital  $SU(N)$  Hubbard model, which can be realized using alkaline-earth-metal cold Fermi gases. Then, we will quickly discuss the symmetries of the model which are useful in capturing the global phase structure. Section III is devoted to the determination of the ground-state phases for strong Kondo coupling. After identifying the ground state in the strong-coupling limit, we derive the low-energy effective Hamiltonians both for ferromagnetic and antiferromagnetic Kondo coupling by taking into account the lowest-order corrections from the kinetic energy. We use these results to prove ferromagnetic ground states in Sec. IV. When  $J_K < 0$ , the effective Hamiltonian satisfies the conditions of the Perron-Frobenius theorem, and ferromagnetism in the ground state

follows immediately. When  $J_K$  is antiferromagnetic, on the other hand, the lowest-order effective Hamiltonian does not resolve the huge  $SU(N)$  “spin” degeneracy. We show that taking into account higher-order corrections lift the degeneracy thereby stabilizing ferromagnetism. We also explain ferromagnetism in the ferromagnetic ( $J_K < 0$ ) Kondo-lattice model by generalizing the double-exchange mechanism to  $SU(N)$ . These are the central results of this paper.

The emergent Bose-Fermi supersymmetry  $SU(N|1)$  in the  $SU(N)$  Kondo-Heisenberg model, which is a variant of the  $SU(N)$  Kondo-lattice model, will be discussed in Sec. V. The main results and some technical details are summarized in Sec. VI and in the Appendixes, respectively.

## II. MODEL

### A. Two-orbital Hubbard model for alkaline-earth-metal cold fermions

To obtain the  $SU(N)$ -symmetric Kondo lattice model, we start from the minimal model that describes the alkaline-earth-metal cold fermions loaded in an optical lattice [4]:

$$\begin{aligned} \mathcal{H}_G &= - \sum_i \sum_{m=g,e} t^{(m)} \sum_{\alpha=1}^N \left( c_{m\alpha,i}^\dagger c_{m\alpha,i+1} + \text{H.c.} \right) \\ &+ \sum_i \sum_{m=g,e} \frac{U^{(m)}}{2} n_{m,i} (n_{m,i} - 1) - \sum_i \sum_{m=g,e} \mu_i^{(m)} n_{m,i} \\ &+ V_H^{g-e} \sum_i n_{g,i} n_{e,i} + V_{\text{ex}}^{g-e} \sum_{i,\alpha\beta} c_{g\alpha,i}^\dagger c_{e\beta,i}^\dagger c_{g\beta,i} c_{e\alpha,i}, \end{aligned} \quad (1)$$

where  $c_{m\alpha,i}^\dagger$  ( $c_{m\alpha,i}$ ) creates (annihilates) a fermion of the color  $\alpha$  ( $= 1, \dots, N$ ) in the “orbital”- $m$  ( $= g, e$ ) at site- $i$ , and  $n_{m,i}$  is the corresponding number operator  $n_{m,i} = \sum_{\alpha} c_{m\alpha,i}^\dagger c_{m\alpha,i}$ . In alkaline-earth-metal cold fermions, the orbital  $g$  ( $e$ ) corresponds to the atomic state  $^1S_0$  ( $^3P_0$ ). The local potential  $\mu_i^{(m)}$  can be site-dependent in general (especially in the cold-atom setting). The interactions  $U^{(m)}$  and  $V_H$  respectively are the Hubbard interactions among the same species of fermions and the density-density interaction between the  $g$  and  $e$  fermions. The last term is the exchange interactions between the fermions in different orbitals, which can be conveniently recast as:

$$- V_{\text{ex}}^{g-e} \sum_i \left( \sum_{A=1}^{N^2-1} \hat{S}_{g,i}^A \hat{S}_{e,i}^A \right) - \frac{1}{N} V_{\text{ex}}^{g-e} \sum_i n_{g,i} n_{e,i} \quad (2)$$

with  $\hat{S}_{g,i}^A$  and  $\hat{S}_{e,i}^A$  being the second-quantized  $SU(N)$  spins for the  $g$  and  $e$  fermions, respectively:

$$\hat{S}_{m,i}^A := \sum_{\alpha,\beta=1}^N c_{m\alpha,i}^\dagger [G^A]_{\alpha\beta} c_{m\beta,i} \quad (m = g, e). \quad (3)$$

The  $N$ -dimensional matrices  $G^A$  ( $A = 1, \dots, N^2 - 1$ ) are the  $SU(N)$  generators normalized as  $\text{Tr}(G^A G^B) = \delta^{AB}$ , and satisfy:

$$\begin{aligned} [G^A, G^B] &= i f^{ABC} G^C \\ \sum_A [G^A]_{\alpha\beta} [G^A]_{\mu\nu} &= \delta_{\alpha\nu} \delta_{\beta\mu} - \delta_{\alpha\beta} \delta_{\mu\nu} / N \\ (\alpha, \beta, \mu, \nu &= 1, \dots, N). \end{aligned} \quad (4)$$

Basically, the exchange interaction  $V_{\text{ex}}^{g-e}$  is the same as the Hund coupling which is ferromagnetic except that here it comes from the atom-atom collision and can be both ferromagnetic and antiferromagnetic. Note that there is no hybridization between the  $g$  and  $e$  fermions which may potentially lead to the mixed-valence physics in heavy-fermion systems [42].

Now we turn off the hopping of the  $e$  fermions:  $t^{(e)} = 0$  while keeping  $t^{(g)}$  finite. Experimentally, this is achieved, e.g., by employing the so-called state-dependent lattice (SDL) [4, 28, 29] in which the  $g$  fermions moving in a shallow lattice remain itinerant while the  $e$  fermions are localized in a deeper lattice [see Fig. 1(a)]. The model parameters can be estimated for actual optical lattices, e.g., for  $^{173}\text{Yb}$  and the setting used in Ref. [29] as:  $t^{(e)}/V_{\text{ex}}^{g-e} \sim 10^{-2}$ ,  $t^{(e)}/t^{(g)} \sim 10^{-3}$ ,  $V_H^{g-e} \simeq V_{\text{ex}}^{g-e}$  ( $> 0$ ),  $U^{(g)}/V_{\text{ex}}^{g-e} \sim 10^{-1}$ ,  $U^{(e)} \simeq V_{\text{ex}}^{g-e}$ , which suggest that we may treat the  $e$ -fermions as localized.

When the deeper lattice sites are uniformly occupied by the  $e$ -fermions, i.e.,  $n_{e,i} = n_e$  ( $= 1, \dots, N$ ), the following  $\frac{N!}{n_e!(N-n_e)!}$ -plet “spin” is formed at each site [43]

$$|[\alpha_1, \dots, \alpha_{n_e}]\rangle = c_{\alpha_1,i}^\dagger \cdots c_{\alpha_{n_e},i}^\dagger |0\rangle$$

(the bracket  $[\dots]$  denotes anti-symmetrization). By the Fermi statistics, these  $SU(N)$  spin states are anti-symmetric in the spin labels  $\{\alpha_k\}$ , and we denote the corresponding irreducible representation (rank- $n_e$  anti-symmetric tensor) by the following Young diagram:

$$n_e \left\{ \begin{array}{|c|} \hline \square \\ \hline \square \\ \hline \square \\ \hline \end{array} \right\}. \quad (5)$$

In what follows, we will frequently use similar Young diagrams as the substitute for the spin “ $S$ ” to specify the  $SU(N)$ -spins (irreducible representations, precisely). For a quick explanation of the Young diagrams and the irreducible representations, see Appendix A (for more details and other useful knowledge of  $SU(N)$ , see, e.g., Ref. [44]).

Under the condition  $n_{e,i} = n_e$  ( $= \text{const.}$ ), the interaction  $V_H^{g-e} \sum_i n_{g,i} n_{e,i}$  in (1) reduces to  $\tilde{V}_H^{g-e} \sum_i n_{g,i} n_{e,i} \rightarrow n_e \tilde{V}_H^{g-e} \sum_i n_{g,i}$  ( $\tilde{V}_H^{g-e} := V_H^{g-e} - V_{\text{ex}}^{g-e}/N$  [45]), which just renormalizes the chemical potential, and can be regarded as a constant in a sector with a fixed fermion number. If we drop the Hubbard interaction  $U^{(g)}$  temporarily, we obtain the following  $SU(N)$  Kondo lattice model (KLM):

$$\begin{aligned} \mathcal{H}_{\text{KLM}} &= -t \sum_i \sum_{\alpha=1}^N \left( c_{\alpha,i}^\dagger c_{\alpha,i+1} + \text{H.c.} \right) + J_K \sum_i \left( \sum_{A=1}^{N^2-1} \hat{S}_i^A \hat{S}_i^A \right), \end{aligned} \quad (6)$$

where we have simplified the notations as:

$$\begin{aligned} c_{\alpha,i}^\dagger &= c_{g\alpha,i}^\dagger, & c_i^\alpha &= c_{g\alpha,i}, & \hat{s}_i^A &= \hat{S}_{g,i}^A, & S_i^A &= \hat{S}_{e,i}^A \\ t &= t^{(g)}, & J_K &= -V_{\text{ex}}^{g-e} \end{aligned} \quad (7)$$

(we shall discuss the effects of the neglected  $U^{(g)}$  in Sec. IV C). Throughout this paper, the number of lattice sites is denoted by  $L$ , and we use  $\mathcal{N}_c$  and  $n_c$  for the total fermion number  $\sum_{i,\alpha} c_{\alpha,i}^\dagger c_i^\alpha = \sum_i n_i$  and the fermion density (or, the average fermion number per site  $\mathcal{N}_c/L$ ), respectively. The fermion filling  $f$  ( $0 \leq f \leq 1$ ) is defined by:  $f = n_c/N$ . Also, unless otherwise stated, we consider only the one-dimensional system with an open boundary condition.

The  $SU(N)$  generalization of the KLM has been originally introduced in the context of spin-orbit-coupled heavy-fermion materials in which  $N$  is the number of the ground-state  $j$ -multiplet ( $N = 2j + 1$ ) and investigated mostly in the large- $N$  limit [46, 47] (for recent finite- $N$  studies, see, e.g., Ref. [48] and references cited therein).

Although the “ $SU(N)$  spin” (the irreducible representation, precisely) of the local moment  $S_i^A$  in (6) is constrained by the fermion statistics to those given by (5) in the cold-atom setting, we can think of arbitrary representations  $\mathcal{R}$  in principle. In what follows, we only consider the case  $n_e = 1$  (exactly one  $e$  atom) at each site, i.e., the local moments in the  $N$ -dimensional representation  $\mathcal{R} = \square$  [which is the  $SU(N)$ -counterpart of  $S = 1/2$ ], as it is the simplest and most realistic in the above cold-gas setting. Note that the situation assumed here is very different from that in the standard large- $N$  treatment [46, 47] in which  $n_e$  is proportional to  $N$ .

In the heavy-fermion setting,  $J_K$  comes from the second-order perturbation in the hybridization between the conduction electron and the localized  $f$ -electron and is bound to be positive and small [49]. In this sense, the large- $J_K$  physics we will consider below is hard to access directly in heavy-fermion systems. On the other hand, if (6) is realized in cold gases, the sign of  $J_K (= -V_{\text{ex}}^{g-e})$  depends on that of the scattering lengths for the  $g$ - $e$  collision [4] and can take both signs, thereby allowing us to explore both ferromagnetic and antiferromagnetic  $SU(N)$  KLM at strong coupling. In fact, it is known experimentally that  $J_K$  is negative (ferromagnetic) for  $^{87}\text{Sr}$  [50] and  $^{173}\text{Yb}$  [51, 52], while it is positive (anti-ferromagnetic) for  $^{171}\text{Yb}$  [53].

We may also add an exchange interaction  $J_H (> 0)$  between the neighboring local spins, which can arise, e.g., from the virtual hopping ( $\sim t^{(e)^2}/U^{(e)}$ ) of the almost localized  $e$  fermions, to define the  $SU(N)$  Kondo-Heisenberg model:

$$\begin{aligned} \mathcal{H}_{\text{KHM}} &= -t \sum_i \sum_{\alpha=1}^N \left( c_{\alpha,i}^\dagger c_{\alpha,i+1} + \text{H.c.} \right) + J_K \sum_i \left( \sum_{A=1}^{N^2-1} \hat{s}_i^A S_i^A \right) \\ &\quad + J_H \sum_i \left( \sum_{A=1}^{N^2-1} S_i^A S_{i+1}^A \right) + V \sum_i n_i n_{i+1}. \end{aligned} \quad (8)$$

In the above, we also have added the density-density interaction  $V$  which may exist (depending on the optical lattice), though the name Kondo-Heisenberg model usually refers to the model with  $V = 0$ . The model (8) will be discussed in Sec. V in the context of the boson-fermion supersymmetry.

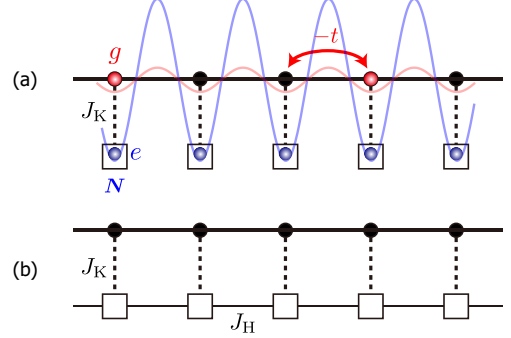


FIG. 1. (a) The  $SU(N)$  Kondo lattice model (6) with the  $SU(N)$  local moments in  $N$  (i.e., the  $N$ -dimensional defining representation  $\square$ ) and its realization with a state-dependent lattice (shown by the red and blue curves). The  $e$ -fermions localized at the bottoms of the deeper lattice play the role of the local moments. (b) The Kondo-Heisenberg model (8) with additional interaction  $J_H$  among the local moments.

## B. Symmetries

### 1. $U(1)$ and $SU(N)$

Now we discuss several symmetries of the models (6) and (8) which will be important in the following discussion. First of all, they are invariant under the following (site-independent)  $U(1)$  gauge transformation for the itinerant fermion:

$$c_i^\alpha \rightarrow e^{i\phi} c_i^\alpha, \quad (9)$$

which is associated with the conservation of the total fermion number:

$$\mathcal{N}_c = \sum_i \sum_{\alpha=1}^N c_{\alpha,i}^\dagger c_i^\alpha.$$

On top of the above  $U(1)$  symmetry, the two models are invariant under the  $SU(N)$  transformation:

$$\begin{aligned} c_i^\alpha &\rightarrow \sum_{\beta=1}^N U(\theta)_{\alpha\beta}^\dagger c_i^\beta \\ S_i^A &\rightarrow \sum_{B=1}^{N^2-1} S_i^B [R_{\text{adj}}(\theta)]_{BA}, \end{aligned} \quad (10)$$

where the transformation  $U(\theta) \in SU(N)$  is defined by

$$U(\theta) := \exp \left( -i \sum_{A=1}^{N^2-1} \theta_A G^A \right),$$

and the adjoint representation  $R_{\text{adj}}(\boldsymbol{\theta}) \in \text{SO}(N^2 - 1)$  is related to  $U$  as:

$$R_{\text{adj}}(\boldsymbol{\theta}) := \exp \left( -i \sum_{A=1}^{N^2-1} \theta_A G_{\text{adj}}^A \right) \\ ([G_{\text{adj}}^A]_{BC} := -if^{ABC}, [G_{\text{adj}}^A]^T = -G_{\text{adj}}^A) .$$

The invariance of the Hamiltonians (6) and (8) can be seen if we note that the  $\hat{U}$  transforms the fermion “spin” as:

$$\hat{s}_i^A \rightarrow \sum_{B=1}^{N^2-1} \hat{s}_i^B [R_{\text{adj}}(\boldsymbol{\theta})]_{BA} . \quad (11)$$

As in  $\text{SU}(2)$ , the  $\text{SU}(N)$ -symmetry leads to several conserved quantities. First, in  $\text{SU}(N)$ , there are  $(N-1)$  commuting generators that play the role of  $S^z$ , and correspondingly, we have a set of the  $(N-1)$  conserved quantities called weight; each state in a given  $\text{SU}(N)$  multiplet has a unique weight [the converse is not true for  $N \geq 3$ ; see Ref. [44] for more details on  $\text{SU}(N)$ ]. In this paper, we denote the local weight associated with  $\hat{s}_i^A + S_i^A$  and its sum over the entire system by  $\lambda_i$  and  $\Lambda_{\text{tot}}$ , respectively. Giving the local weight  $\lambda_i$  and the local fermion number  $n_i + 1$  (1 from the localized  $e$  fermion,  $0 \leq n_i \leq N$ ) is equivalent to specifying the color-resolved fermion density  $n_{\alpha,i} = \sum_{m=g,e} c_{m\alpha,i}^\dagger c_{m\alpha,i}$  ( $\alpha = 1, \dots, N$ ). On top of the weight, there are  $N-1$  Casimir operators  $\mathcal{C}_2, \dots, \mathcal{C}_N$  that are the  $\text{SU}(N)$  analog of the spin squared  $S^2$ . Among them, the quadratic Casimir  $\mathcal{C}_2$  defined in Appendix B is crucial in evaluating the Kondo energies.

## 2. Particle-hole transformation

The particle-hole (P-H) transformation that interchanges the creation and annihilation operators for the itinerant fermions:

$$c_i^\alpha \leftrightarrow c_{\alpha,i}^\dagger \quad (\alpha = 1, \dots, N) \quad (12)$$

plays a key role to understand the global phase structure of the  $N = 2$  KLM. The first hallmark of the  $\text{SU}(N \geq 3)$  KLM is the *absence* of the particle-hole symmetry, as we will see below. By the P-H transformation (12), physical quantities transform as:

$$n_i = \sum_{\alpha} n_{i,\uparrow} \xrightarrow{\text{P-H}} N - n_i \quad \left( f := n_c/N \xrightarrow{\text{P-H}} 1 - f \right) \quad (13a)$$

$$\hat{s}_i^A \xrightarrow{\text{P-H}} \sum_{\sigma,\sigma'} c_{\beta,i}^\dagger [-(G^A)^T]_{\beta\alpha} c_i^\alpha =: \hat{\bar{s}}_i^A \quad (13b)$$

$$\left( c_{\alpha,i}^\dagger c_j^\alpha + c_{\alpha,j}^\dagger c_i^\alpha \right) \xrightarrow{\text{P-H}} - \left( c_{\alpha,i}^\dagger c_j^\alpha + c_{\alpha,j}^\dagger c_i^\alpha \right) . \quad (13c)$$

The third equation implies that the P-H transformation flips the sign of the hopping term

$$t_{i,j} \xrightarrow{\text{P-H tr}} -t_{i,j} , \quad (14)$$

which is not important on bipartite lattices as we can always undo the minus sign by applying the gauge transformation (9) with  $\phi = \pi$  only on one of the sublattices. The equation (13b) tells that the  $\text{SU}(N)$ -spin (of the itinerant fermions)  $\hat{s}_i$  maps onto its conjugate:

$$\hat{s}_i \xrightarrow{\text{P-H tr}} \hat{\bar{s}}_i ,$$

which in general is different from  $\hat{s}_i$  for  $N \geq 3$  (see Appendix A for the conjugate representations). Therefore, the Kondo coupling changes its form by the particle-hole transformation:

$$\sum_{A=1}^{N^2-1} \hat{s}_i^A S_i^A \xrightarrow{\text{P-H tr}} \sum_{A=1}^{N^2-1} \hat{\bar{s}}_i^A S_i^A \left( \neq \sum_{A=1}^{N^2-1} \hat{s}_i^A S_i^A \right) \quad (15)$$

for  $N \geq 3$  [54]. However, if we simultaneously replace the local spin with its conjugate

$$S_i^A \xrightarrow{\text{conjugate}} \bar{S}_i^A = -(S_i^A)^T , \quad (16)$$

the Kondo coupling changes to

$$\sum_{A=1}^{N^2-1} \hat{s}_i^A S_i^A \xrightarrow{\text{P-H}} \sum_{A=1}^{N^2-1} \hat{\bar{s}}_i^A S_i^A \xrightarrow{\text{conjugate}} \sum_{A=1}^{N^2-1} \hat{\bar{s}}_i^A \bar{S}_i^A . \quad (17)$$

As the quadratic Casimirs for an irreducible representation (“spin”)  $\mathcal{R}$  and its conjugate  $\bar{\mathcal{R}}$  are the same, the two different Kondo couplings  $\sum_A \hat{s}_i^A S_i^A$  and  $\sum_A \hat{\bar{s}}_i^A \bar{S}_i^A$  share the same set of the eigenvalues. Therefore, the particle-hole transformation relates the  $\text{SU}(N)$  KLM at filling  $f$  with the local spins  $\mathcal{R}$  to the same model at filling  $1 - f$  with the conjugate local spins  $\bar{\mathcal{R}}$  (see Fig. 2):

$$\mathcal{H}_{\text{KLM}}(t_{i,j}, J_K, f; \mathcal{R}) \xleftrightarrow{\text{P-H tr}} \mathcal{H}_{\text{KLM}}(-t_{i,j}, J_K, 1 - f; \bar{\mathcal{R}}) \quad (18)$$

which means that the ground state of the KLM with local moments in  $\mathcal{R}$  at filling  $f$  is obtained from that of *another* KLM with local moments  $\bar{\mathcal{R}}$  at filling  $1 - f$  by particle-hole transformation, and vice versa. Only for self-conjugate local spins ( $\bar{\mathcal{R}} = \mathcal{R}$ ), particle-hole symmetry exists guaranteeing the symmetry of the phase diagram with respect to the half-filling  $f = 1/2$ .

## III. STRONG-COUPLING LIMITS

In this section, we derive the effective Hamiltonians describing the low-energy physics of the  $\text{SU}(N)$  KLM (6) in the limit of large  $|J_K|$ . Throughout this and the next section IV, we only consider the pure KLM (6) [or the model (8) with  $J_H = V = 0$ ].

### A. Strong-coupling ground state

To carry out the strong-coupling ( $t/J_K$ ) expansion, it is necessary to first evaluate the local Kondo energy

$$J_K \sum_{A=1}^{N^2-1} \hat{s}_i^A S_i^A =: J_K \hat{\mathbf{s}}_i \cdot \mathbf{S}_i . \quad (19)$$



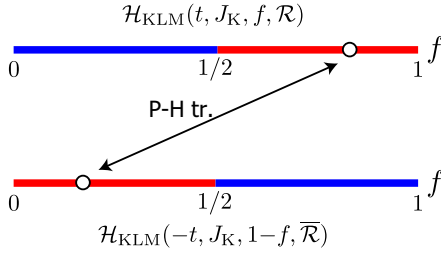


FIG. 2. Particle-hole transformation for  $SU(N)$  Kondo lattice model (6). When the local moments are not self-conjugate,  $SU(N)$  Kondo lattice model with local moments  $\mathcal{R}$  is mapped onto *another* model in which the local moments are replaced with the conjugate ones  $\overline{\mathcal{R}}$ .

As in the standard  $SU(2)$  case, the value depends on the fermion number  $n = \sum_{\alpha} c_{\alpha}^{\dagger} c_{\alpha}$  and how the fermion spin  $\hat{s}_i$  and the local moment  $\mathbf{S}_i$  are combined into the total  $SU(N)$  spin. When the fermion number is  $n_c$  ( $n_c = 1, \dots, N-1$ ), the following two “total spins” are possible [see Eq. (B4)]:

$$n_{c+1} \left\{ \begin{array}{|c|} \hline \square \\ \hline \end{array} \right\}, \quad n_c \left\{ \begin{array}{|c|} \hline \square \\ \hline \end{array} \right\} \quad (1 \leq n_c \leq N-1). \quad (20)$$

When  $n_c = 0$  (empty) and  $n_c = N$  (fully-occupied), the itinerant fermions are in the  $SU(N)$ -singlets and only the local spin contributes to the total spin:

$$\bullet \otimes \square \sim \square \quad (N\text{-rep.}). \quad (21)$$

fermions      local moment

The Kondo energies  $e_K(n_c)$  for these states are calculated using the quadratic Casimir  $\mathcal{C}_2$  introduced in Appendix B:

$$\begin{aligned} e_K(n_c) &= -\frac{N+1}{N} n_c J_K \quad \text{for } n_{c+1} \left\{ \begin{array}{|c|} \hline \square \\ \hline \end{array} \right\}, \\ e_K(n_c) &= \left(1 - \frac{n_c}{N}\right) J_K \quad \text{for } n_c \left\{ \begin{array}{|c|} \hline \square \\ \hline \end{array} \right\} \quad (1 \leq n_c \leq N-1) \\ e_K(n_c) &= 0 \quad (n_c = 0, N). \end{aligned} \quad (22)$$

The results are summarized in Table I. The Kondo energies are plotted in Fig. 3 for  $N = 2$  and  $N = 4$  against the fermion number (per site)  $n_c$ . When  $N = 2$ , the energy is symmetric with respect to  $n_c = 1$  (half-filling) reflecting the particle-hole symmetry, while for  $N = 4$ , this symmetry is lost. It is well-known [40] that, for  $SU(2)$ , a single fermion (electron) and an  $S = 1/2$  moment can form a spin-singlet called the Kondo singlet. However, a local spin in the  $N$  ( $\square$ ) representation cannot be screened by a single fermion, and in fact we need  $N-1$  fermions to make an  $SU(N)$  singlet [see Fig. 3(b)]. With this caution in mind, we take over the name *Kondo singlet* to denote this  $SU(N)$  singlet state formed by  $(N-1)$  fermions and a local spin.

Now let us determine the strong-coupling ground state by minimizing the total Kondo energy  $\sum_i J_K \hat{s}_i \cdot \mathbf{S}_i$ . To this end, we start from the reference state in which the local fermion number  $n_c$  is integer and uniform. For  $1 \leq n_c \leq N-1$ , the states in  $n_{c+1} \left\{ \begin{array}{|c|} \hline \square \\ \hline \end{array} \right\}$  and  $n_c \left\{ \begin{array}{|c|} \hline \square \\ \hline \end{array} \right\}$  are selected *at each site*

for  $J_K > 0$  and  $J_K < 0$ , respectively. Naively, the strong-coupling ground state may be obtained by uniformly tiling one of these two according to the sign of  $J_K$ . However, this strategy works only when  $n_c = N-1$  (for  $J_K > 0$ ) or  $n_c = 1$  (for  $J_K < 0$ ) at which the Kondo energy  $e_K(n_c)$  is concave (see Fig. 3). The linear behavior of the Kondo energy for other  $n_c$  means that we can move one fermion from one site to another  $[(n_c, n_c) \rightarrow (n_c + 1, n_c - 1)]$  without changing the Kondo energy of the entire system. Repeating this procedure, we can generate many *inhomogeneous* ground states which are degenerate with the uniform one. Physically, we may expect that the (strong-coupling) ground states at these commensurate fillings  $f (= n_c/N)$  are metallic.

In what follows, we restrict ourselves to the two regions

$$\begin{aligned} \text{(i)} \quad & 0 \leq f \leq 1/N \quad (J_K < 0) \\ \text{(ii)} \quad & 1 - 1/N \leq f \leq 1 \quad (J_K > 0) \end{aligned} \quad (23)$$

in which the strong-coupling ground state is well under control. Specifically, in the case (i), each site is occupied either by  $\square$  ( $n_c = 0$ ) or by  $\square$  ( $n_c = 1$ ) as is shown in Fig. 4(a,b), while in (ii), only the Kondo singlet  $\bullet$  ( $n_c = N-1$ ) and the  $N$ -dimensional “spin”  $\square$  ( $n_c = N$ ) appear in the ground states [see Fig. 6(a,c)]. In particular, when  $J_K < 0$ , the (spin-degenerate) ground states at the commensurate filling  $f = 1/N$  ( $n_c = 1$  fermion at each site) are given by a uniform tiling of the state  $\square$  [Fig. 4(a)]. When  $J_K > 0$ , on the other hand, the ground state at  $f = 1 - 1/N$  ( $n_c = N-1$ ) is the tensor product of the Kondo singlets [Fig. 6(a)] and is non-degenerate.

TABLE I. List of all the  $2^N \times N$  on-site states and their Kondo energies.

fermion num.	total spin	Kondo energy	degeneracy
$n_c = 0$ (empty)	$\square$	0	$N$
$1 \leq n_c \leq N-1$	$n_c \left\{ \begin{array}{ c } \hline \square \\ \hline \end{array} \right\}$ $n_{c+1} \left\{ \begin{array}{ c } \hline \square \\ \hline \end{array} \right\}$	$\left(1 - \frac{n_c}{N}\right) J_K$ $-\frac{N+1}{N} n_c J_K$	$\frac{n_c(N+1)!}{(n_c+1)!(N-n_c)!}$ $\frac{N!}{(n_c+1)!(N-n_c-1)!}$
$n_c = N$ (fully-occupied)	$\square$	0	$N$

## B. Ferromagnetic Kondo coupling

### 1. Insulating phase at $f = 1/N$ ( $n_c = 1$ )

Having found the ground states at  $t = 0$ , let us consider the excited states at the commensurate filling  $f = 1/N$ . The energy cost by the addition of one fermion [Fig. 4(b)] is calculated as

$$\Delta_c^+ = -J_K/N = |J_K|/N, \quad (24)$$

while, when a fermion is removed [see Fig. 4(c)], the cost is given by:

$$\Delta_c^- = -(N-1)J_K/N = (N-1)|J_K|/N. \quad (25)$$

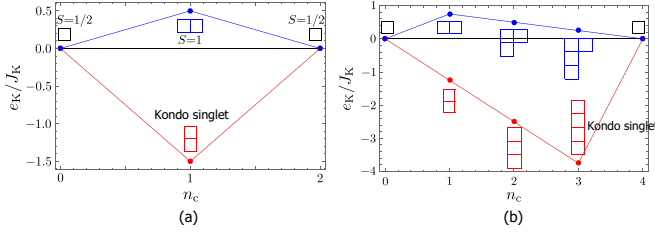


FIG. 3. Kondo energies (22) vs. fermion number  $n_c$  ( $0 \leq n_c \leq N$ ) for (a)  $N = 2$  and (b)  $N = 4$  (red for anti-symmetric  $(n_c + 1)$ -tensor representation). Note that when  $N = 2$  [i.e.,  $SU(2)$ ], the Kondo energy is symmetric with respect to  $n_c = N/2 = 1$  as a consequence of the particle-hole symmetry, while this symmetry is lost for  $N \geq 3$ .

The two gaps are different for  $N \geq 3$  as a consequence of the absence of particle-hole symmetry. To move one fermion from one site to another [Fig. 4(d)], we need extra energy:

$$\Delta_c^{P-H} = (1 - 2/N)J_K - 2 \times (1 - 1/N)J_K = -J_K = |J_K|. \quad (26)$$

The three energies satisfy:

$$\Delta_c^+ \leq \Delta_c^- < \Delta_c^{P-H} \quad (27)$$

(the equalities hold when  $N = 2$ ). Therefore, we may expect that an insulating ground state forms at  $1/N$ -filling (i.e.,  $n_c = 1$ ).

One may naively create the spin excitation by turning one of the  $\square\square$  spins in Fig. 4(a) into  $\square$ . However, this may not be the lowest spin excitation. The behavior of the  $SU(N)$  spin-sector is non-trivial as the strong-coupling ( $t = 0$ ) ground state is highly degenerate (the degree of degeneracy is  $[N(N+1)/2]^L$ ) with respect to the  $SU(N)$  spin states. The second-order degenerate perturbation in  $t$  yields the following effective  $SU(N)$  Heisenberg Hamiltonian for the spin sector:

$$\mathcal{H}_{\text{eff}} = \frac{t^2}{2|J_K|} \sum_i \mathcal{S}_i^A(\square\square) \mathcal{S}_{i+1}^A(\square\square), \quad (28)$$

with the spins  $\mathcal{S}_i$  belonging to the symmetric rank-2 tensor  $\square\square$  [when  $N = 2$ , (28) reduces to the spin-1 Heisenberg chain]. The inclusion of the  $J_H$ -interaction merely renormalizes the coupling:  $\frac{t^2}{2|J_K|} \rightarrow \frac{t^2}{2|J_K|} + J_H/4$ . According to the recent analytical and numerical studies [55–57], the low-energy physics of the model (28) depends on the parity of  $N$ . That is, the strong coupling  $SU(N)$  Kondo lattice model (6) at filling  $f = 1/N$  is a spin-gapped insulator when  $N$  is even, while it is an insulator with algebraic spin correlations when  $N$  is odd. Except when  $N = 2$ , these spin-gapped insulators for  $N = \text{even}$  are not the symmetry-protected topological phases associated with  $PSU(N)$  [58].

## 2. Effective Hamiltonian for $0 \leq f \leq 1/N$

When we move away from the commensurate filling  $f = 1/N$ , the strong-coupling ground states now contain a certain

number of sites in  $\square$  ( $n_c = 0$ ) as well as those in  $\square\square$  [see Fig. 5(a-1,2)]. These ground states are highly degenerate with respect not only to the locations of the  $\square$  spins in the “sea” of  $\square\square$  but also to the  $SU(N)$  spin states at the individual sites. This huge degeneracy might be partially or fully resolved by the motion of the fermions.

To understand how the degeneracy is lifted, let us derive an effective Hamiltonian within the ground-state subspace by the first-order perturbation in  $t$ . To this end, we need to find the expression of the hopping term projected onto the ground-state manifold. To begin with, we explicitly write the expressions of the spin states in  $\square$  and  $\square\square$ . As the fermionic (F) part of the states with  $n_c = 0$  (empty) and  $n_c = 1$  are given respectively by:

$$\begin{aligned} n_c = 0 : & \quad |0\rangle_F \\ n_c = 1 : & \quad |\alpha\rangle_{F,i} := c_{\alpha,i}^\dagger |0\rangle_F \quad (\alpha = 1, \dots, N), \end{aligned} \quad (29)$$

the two types of spin states are given by (“S” stands for the local-spin part of the state):

$$|N; \alpha\rangle_i = |\alpha\rangle_{S,i} \otimes |0\rangle_F \quad (n_c = 0, \square\text{-spin}) \quad (30a)$$

and

$$\begin{aligned} |(\alpha, \beta)\rangle_i &= \begin{cases} |\alpha\rangle_{S,i} \otimes c_{\alpha,i}^\dagger |0\rangle_F & (\alpha = \beta) \\ \frac{1}{\sqrt{2}} \{ |\alpha\rangle_{S,i} \otimes c_{\beta,i}^\dagger |0\rangle_F + |\beta\rangle_{S,i} \otimes c_{\alpha,i}^\dagger |0\rangle_F \} & (\alpha < \beta) \end{cases} \\ & \quad (n_c = 1, \square\square\text{-spin}). \end{aligned} \quad (30b)$$

When no fermion occupies a pair of adjacent sites ( $i, i+1$ ), the hopping term simply annihilates the state. If each of the pair is occupied by one fermion (i.e.,  $\square\square - \square\square$ ), the action of the hopping always creates excited states:

$$\begin{aligned} |\square\square\rangle_i \otimes |\square\square\rangle_{i+1} &\xrightarrow{c_{\mu,i+1}^\dagger c_i^\mu} |\square\rangle_i \otimes |\square\square\rangle_{i+1} \quad (\Delta E = |J_K|) \\ |\square\square\rangle_i \otimes |\square\square\rangle_{i+1} &\xrightarrow{c_{\mu,i}^\dagger c_{\mu+1}^\mu} |\square\square\rangle_i \otimes |\square\rangle_{i+1} \quad (\Delta E = |J_K|) \end{aligned} \quad (31)$$

and does not contribute to the first-order perturbation. Therefore, only the pairs of the form  $\square\square - \square$  or  $\square - \square\square$  can contribute to the effective Hamiltonian. To investigate the action of the hopping operator onto the above pair, it is convenient to use the following expressions of the fermion operators  $\tilde{c}_i^\alpha$  and  $\tilde{c}_{\alpha,i}^\dagger$  projected onto the ground-state manifold:

$$\begin{aligned} \tilde{c}_i^\alpha &= |N; \alpha\rangle_i \langle(\alpha, \alpha)|_i \\ &+ \frac{1}{\sqrt{2}} \sum_{\beta < \alpha} |N; \beta\rangle_i \langle(\beta, \alpha)|_i + \frac{1}{\sqrt{2}} \sum_{\beta > \alpha} |N; \beta\rangle_i \langle(\alpha, \beta)|_i \\ \tilde{c}_{\alpha,i}^\dagger &= |(\alpha, \alpha)\rangle_i \langle N; \alpha|_i \\ &+ \frac{1}{\sqrt{2}} \sum_{\beta < \alpha} |(\beta, \alpha)\rangle_i \langle N; \beta|_i + \frac{1}{\sqrt{2}} \sum_{\beta > \alpha} |(\alpha, \beta)\rangle_i \langle N; \beta|_i. \end{aligned} \quad (32)$$

In writing the effective Hamiltonian, we also need to keep track of the sign factors arising from the fermion exchange. Fortunately, for open boundary conditions, no extra sign appears in the subspace considered here, and we obtain the following effective Hamiltonian:

$$\begin{aligned}
 & -t \sum_{\mu=1}^N \tilde{c}_{\mu,i}^\dagger \tilde{c}_j^\mu \underbrace{|N; \alpha\rangle_i}_{\square} \otimes \underbrace{|(\beta, \gamma)\rangle_j}_{\square} \\
 & = \begin{cases} -\frac{t}{\sqrt{2}} |(\alpha, \beta)\rangle_i \otimes |N; \beta\rangle_j - \frac{t}{\sqrt{2}} (\sqrt{2}-1) \delta_{\alpha\beta} |(\alpha, \alpha)\rangle_i \otimes |N; \alpha\rangle_j & \text{when } \beta = \gamma \\ -\frac{t}{2} |(\alpha, \gamma)\rangle_i \otimes |N; \beta\rangle_j - \frac{t}{2} |(\alpha, \beta)\rangle_i \otimes |N; \gamma\rangle_j & \text{when } \beta \neq \gamma. \end{cases} \quad (33) \\
 & \quad -\frac{t}{2} (\sqrt{2}-1) \delta_{\alpha\gamma} |(\alpha, \alpha)\rangle_i \otimes |N; \beta\rangle_j - \frac{t}{2} (\sqrt{2}-1) \delta_{\alpha\beta} |(\alpha, \alpha)\rangle_i \otimes |N; \gamma\rangle_j
 \end{aligned}$$

Obviously, all the non-zero off-diagonal matrix elements appearing here are negative when  $t > 0$ . In the cold-atom realization,  $t$  is positive and this condition is satisfied from the outset. When the system is periodic, hopping across the boundary yields a fermion sign  $(-1)^{N_c-1}$  that necessitates an additional condition  $N_c = \text{odd}$  for the non-positivity.

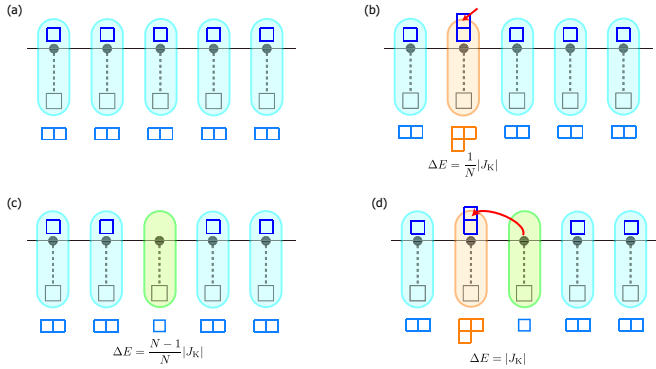


FIG. 4. Ground and excited states in the strong-coupling limit when the Kondo interaction is ferromagnetic ( $J_K < 0$ ). (a) Singlet ground state, (b) single-particle excitation, (c) “hole” excitation, and (d) particle-hole excitation. Red ovals denote “Kondo singlets”.

### C. Antiferromagnetic Kondo coupling

#### 1. Insulating phase at $f = 1 - 1/N$

As has been discussed in Sec. III A, the strong-coupling ground state when  $f = 1 - 1/N$  (or  $n_c = N - 1$  fermions at each site) and  $J_K > 0$  is the product of the local Kondo singlets shown in Fig. 6(a) and is non-degenerate. Adding (removing) one fermion to (from) this ground state costs finite energy [Fig. 6(b)]

$$\Delta_c^+ = (N^2 - 1)J_K/N \quad [\Delta_c^- = (N + 1)J_K/N]. \quad (34)$$

The addition always costs more energy, i.e.,  $\Delta_c^+ - \Delta_c^- = (N+1)(N-2)J_K/N > 0$  when  $N \geq 3$  (due to the absence of the particle-hole symmetry). On the other hand, moving one fermion from one site to another [particle-hole excitations; see Fig. 6(c)] also costs an energy

$$\Delta_c^{\text{P-H}} = (N + 1)J_K. \quad (35)$$

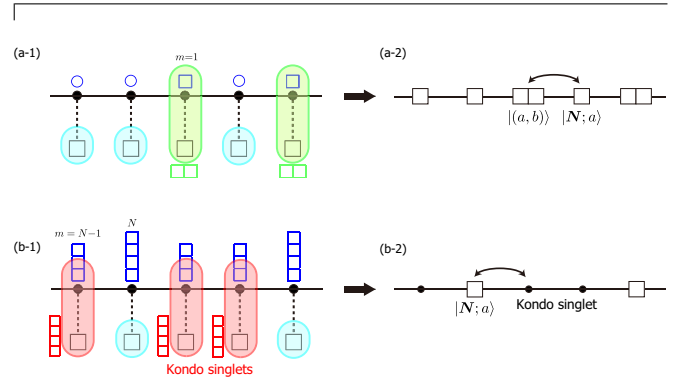


FIG. 5. Ground states in the strong-coupling limit at partial filling  $0 \leq n_c \leq 1$  when  $J_K < 0$  (a-1) and  $N - 1 \leq n_c \leq N$  when  $J_K > 0$  (b-1). The ground-state subspace is spanned by  $N$  and the rank-2 symmetric tensor (Kondo singlets  $\bullet$  and  $N$ ) in (a) [(b)]. The corresponding effective Hamiltonians within the ground-state subspaces are shown in (a-2) and (b-2).

To create a “spin” excitation in the ground state, one needs to excite one of the  $SU(N)$  Kondo singlets to the adjoint [see Fig. 6(d)]:

$$N \left\{ \begin{array}{c} \square \\ \square \end{array} \right\} \rightarrow N-1 \left\{ \begin{array}{c} \square \\ \square \end{array} \right\}. \quad (36)$$

The energy cost of this “magnetic” excitation is  $\Delta_s = NJ_K$ . These imply that for large enough  $J_K (> 0)$ , the ground state of  $\mathcal{H}_{\text{KLM}}$  (6) at  $f = 1 - 1/N$  is a spin-gapped insulator, which is the  $SU(N)$  analog of the well-known Kondo insulator at half-filling in the  $SU(2)$  KLM [59].

#### 2. Effective Hamiltonian for $1 - 1/N \leq f \leq 1$

Now let us find the effective Hamiltonian which is first-order in  $t$ . The ground-state manifold in this region is spanned

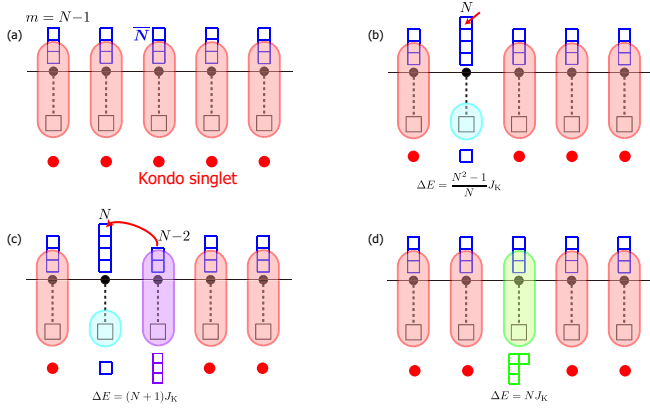


FIG. 6. Ground and gapped excited states in the strong-coupling limit ( $J_K > 0$ ). (a) Singlet ground state, (b) single-particle excitation, (c) particle-hole excitation, and (d) “spin” excitation. Red ovals denote “Kondo singlets”.

by the following two types of fermion states:

$$\begin{aligned}
 n_c = N : \quad |f\rangle_{F,i} &:= \prod_{\beta=1}^N c_{i,\beta}^\dagger |0\rangle_F = c_{i,1}^\dagger \cdots c_{i,N}^\dagger |0\rangle_F \\
 n_c = N - 1 : \quad |\alpha\rangle_{F,i} &:= c_i^\alpha |f\rangle_{F,i} = (-1)^{\alpha-1} \prod_{\beta \neq \alpha} c_{i,\beta}^\dagger |0\rangle_F.
 \end{aligned} \quad (37)$$

Due to the strong  $J_K > 0$ , the above states with  $n_c = N - 1$  (conjugate  $\bar{N}$ ) and  $n_c = N$  (singlet), together with the local moment in  $N$ , form the  $SU(N)$  multiplets in  $\bullet$  (Kondo singlet) and  $N$  ( $\square$ ), respectively [see Fig. 5(b-2)]. Written explicitly, these multiplets are given as:

$$|\bullet\rangle_i := \frac{1}{\sqrt{N}} \sum_{\alpha=1}^N |\alpha\rangle_{S,i} \otimes |\alpha\rangle_{F,i} = \frac{1}{\sqrt{N}} \sum_{\alpha=1}^N |\alpha\rangle_{S,i} \otimes c_i^\alpha |f\rangle_{F,i} \quad (38a)$$

when  $m = N - 1$ , and

$$|N; \alpha\rangle_i := |\alpha\rangle_{S,i} \otimes |f\rangle_{F,i} \quad (\alpha = 1, \dots, N) \quad \text{when } m = N, \quad (38b)$$

where  $|\alpha\rangle_{S,i}$  denotes the states of the local spin in  $N$ . When  $n_c = N - 1$ , there is yet another multiplet in the adjoint representation ( $N-1$   $\left\{ \begin{smallmatrix} \square & \square \\ \square & \square \end{smallmatrix} \right\}$ ):

$$|\text{adj}; A\rangle_i = \sum_{\alpha, \beta=1}^N [G^A]^\alpha_\beta |\alpha\rangle_{S,i} \otimes |\beta\rangle_{F,i}, \quad (39)$$

which is not allowed energetically in the ground state when  $J_K$  is positively large but is necessary for considering the higher-order corrections in Sec. IV B 2.

It is straightforward to write the expressions of the fermion operators projected onto the subspace spanned by the above two states (38a) and (38b), which are given (up to the many-body fermion sign) by:

$$\tilde{c}_{\alpha,i}^\dagger = \frac{1}{\sqrt{N}} |N; \alpha\rangle_i \langle \bullet|_i, \quad \tilde{c}_i^\alpha = \frac{1}{\sqrt{N}} |\bullet\rangle_i \langle N; \alpha|_i. \quad (40)$$

Note that they now obey the non-standard anti-commutation relations:

$$\begin{aligned}
 \{\tilde{c}_i^\alpha, \tilde{c}_i^\beta\} &= \{\tilde{c}_{\alpha,i}^\dagger, \tilde{c}_{\beta,i}^\dagger\} = 0 \\
 \{\tilde{c}_i^\alpha, \tilde{c}_{\beta,i}^\dagger\} &= \frac{1}{N} \delta^\beta_\alpha |\bullet\rangle_i \langle \bullet| + \frac{1}{N} |N; \alpha\rangle_i \langle N; \beta|.
 \end{aligned} \quad (41)$$

We will see in Sec. V that these commutation relations are closely related to Bose-Fermi supersymmetry.

If we use the following for the fermionic part of the many-body basis states

$$\begin{aligned}
 &|i_1^{\alpha_1}, i_2^{\alpha_2}, \dots, i_n^{\alpha_n}\rangle_F \\
 &= \prod_{k=1}^n (-1)^{(N-1)i_k} |\dots\rangle_F \otimes |\alpha_1\rangle_{F,i_1} \otimes \dots \otimes |\alpha_n\rangle_{F,i_n} \otimes |\dots\rangle_F,
 \end{aligned} \quad (42)$$

the effective Hamiltonian (up to the first order in  $t$ ) is given by:

$$-t \sum_{\beta=1}^N \tilde{c}_{\beta,i+1}^\dagger \tilde{c}_i^\beta |\dots\rangle \otimes |N; \alpha\rangle_i \otimes |\bullet\rangle'_{i+1} \otimes |\dots\rangle \quad (43a)$$

$$\begin{aligned}
 &= -\frac{t}{N} |\dots\rangle \otimes |\bullet\rangle'_i \otimes |N; \alpha\rangle_{i+1} \otimes |\dots\rangle, \\
 &-t \sum_{\beta=1}^N \tilde{c}_{\beta,i}^\dagger \tilde{c}_{i+1}^\beta |\dots\rangle \otimes |\bullet\rangle'_i \otimes |N; \alpha\rangle_{i+1} \otimes |\dots\rangle \\
 &= -\frac{t}{N} |\dots\rangle \otimes |N; \alpha\rangle_i \otimes |\bullet\rangle'_{i+1} \otimes |\dots\rangle,
 \end{aligned} \quad (43b)$$

with  $|\bullet\rangle'_i$  now being defined by:

$$|\bullet\rangle'_i := (-1)^{(N-1)i} \frac{1}{\sqrt{N}} \sum_{\alpha=1}^N |\alpha\rangle_{S,i} \otimes c_i^\alpha |f\rangle_{F,i}. \quad (44)$$

The extra sign factor  $(-1)^{(N-1)i}$  in Eqs. (42) and (44) has been introduced to eliminate the many-body fermion sign.

#### IV. FERROMAGNETISM

In this section, we prove that the ground state of the  $SU(N)$  KLM (6) is ferromagnetic in the two regions considered in the previous section. Before doing so, we first characterize the ferromagnetic states in  $SU(N)$ -symmetric systems in physical terms. In the ordinary  $SU(2)$ -symmetric systems, the standard intuitive picture of ferromagnetic states is that all the spins depicted as arrows are aligned in a particular direction. In general, this simple picture holds only in  $SU(2)$  where all the spin- $S$  can be represented by the (symmetrized) product of  $2S$  spin- $1/2$ s and any  $S = 1/2$  states can be uniquely represented by points on the unit sphere. In  $SU(N)$ , even a pair of  $SU(N)$  “spins” that are coupled ferromagnetically may not point in the same direction. Nevertheless, in the situations considered here (i.e.,  $N$ -component fermions coupled to  $N$ -component local spins), we can use, instead of the three-component unit



vector in  $SU(2)$ , a complex unit vector  $\mathbf{z} = (z_1, \dots, z_N)$  to uniquely specify the state of a single  $N$ -component fermion (for both itinerant and localized fermions) [60]; the coincidence of  $\mathbf{z}$  up to phases means the same  $SU(N)$  spin state and the same spin  $\langle S^A \rangle$  [see Fig. 7(b) and Eq. (56)]. As will be seen in Sec. IV D, the coherent state  $|\mathbf{z}\rangle$  specified by the complex vector  $\mathbf{z}$  coincides with the “fully-polarized” state  $|1\rangle = c_1^\dagger|0\rangle$  up to  $SU(N)$  rotation. Therefore, we may think of the ferromagnetic state in the present cases as the one in which *all* the constituent  $SU(N)$  spins  $\square$  (both itinerant and local; the spins  $\square$  are treated as made of two  $\square$ ’s) are in the same state, e.g.,  $|1\rangle$  [ $\mathbf{z} = (1, 0, \dots, 0)$ ; see Fig. 7(c)] and those obtained from it by applying the  $SU(N)$  lowering operators.

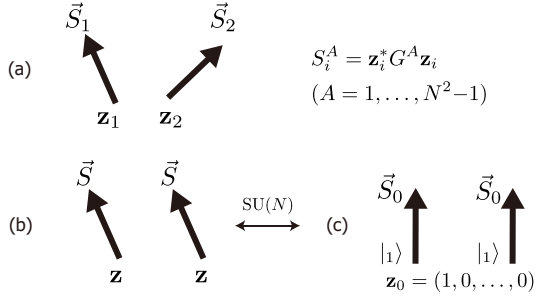


FIG. 7. Semiclassical (coherent-state) representation of the states  $|\mathbf{z}\rangle$  of  $SU(N)$  “spins” ( $\square$ ) and the corresponding  $SU(N)$  moment  $\vec{S}$ . Generic configuration (a) and ferromagnetic ones (b,c). The  $SU(N)$  “spin” moment is represented by an  $(N^2 - 1)$ -dimensional (real) vector  $\vec{S} = (S^1, \dots, S^{N^2-1})$  given by  $S^A = \mathbf{z}^\dagger G^A \mathbf{z}$  [see Eq. (56)].

#### A. Ferromagnetism in low-density region $0 < f < 1/N$

As we have seen, the strong-coupling effective Hamiltonian (33) for large ferromagnetic  $J_K$  is given by a non-positive matrix when  $t > 0$ . Of course, as the effective Hamiltonian (33) preserves the total  $SU(N)$  weight, the full effective Hamiltonian for an  $L$ -site system decomposes into several blocks with respect to the conserved weight  $\Lambda_{\text{tot}}$ . In the following, we consider one of those blocks with a given total  $SU(N)$  weight  $\Lambda_{\text{tot}}$ , which we denote by  $\mathcal{H}_{\text{eff}}(\Lambda_{\text{tot}}; L)$ . To prove ferromagnetism, we need one more important property called irreducibility or indecomposability on top of the non-positivity. A given real Hamiltonian matrix  $\mathcal{H}$  is said irreducible if there exists a sequence of non-zero off-diagonal matrix elements  $\mathcal{H}_{ik_{n-1}} \mathcal{H}_{k_{n-1}k_{n-2}} \cdots \mathcal{H}_{k_1j}$  ( $n \geq 1$ ) for any pair of  $(i, j)$  ( $i \neq j$ ). Physically, this implies that repeated application of  $\mathcal{H}$  can connect any pair of the initial ( $j$ ) and final ( $i$ ) states. For simplicity of the argument, we assume the open boundary condition [61]. Then, it is straightforward to show, by the mathematical induction, that the block Hamiltonian  $\mathcal{H}_{\text{eff}}(\Lambda_{\text{tot}}; L)$  is irreducible (see Appendix C for the sketch of the proof).

Now, by the Perron-Frobenius theorem (see, e.g., Ref. [62] for a physicist-friendly exposition of the theorem), we can

prove that the ground state  $|\Psi_{\text{g.s.}}(\Lambda_{\text{tot}})\rangle$  of  $\mathcal{H}_{\text{eff}}(\Lambda_{\text{tot}}; L)$  is unique and is given by a superposition of all the possible tensor-products of the states (30a) and (30b) (allowed for the value of  $\Lambda_{\text{tot}}$ ) with strictly positive coefficients. Obviously, the ferromagnetic states [with the same  $SU(N)$  weight  $\Lambda_{\text{tot}}$ ] have a similar sign property, which implies

$$\mathcal{P}_{\text{ferro}}(\Lambda_{\text{tot}})|\Psi_{\text{g.s.}}(\Lambda_{\text{tot}})\rangle \neq 0 \quad (45)$$

with  $\mathcal{P}_{\text{ferro}}(\Lambda_{\text{tot}})$  being the projector onto the ferromagnetic states in the subspace with  $\Lambda_{\text{tot}}$ . Since the block Hamiltonian  $\mathcal{H}_{\text{eff}}(\Lambda_{\text{tot}}; L)$  commutes with  $\mathcal{P}_{\text{ferro}}(\Lambda_{\text{tot}})$ , we immediately see that  $\mathcal{P}_{\text{ferro}}(\Lambda_{\text{tot}})|\Psi_{\text{g.s.}}(\Lambda_{\text{tot}})\rangle$  is a ground state of  $\mathcal{H}_{\text{eff}}(\Lambda_{\text{tot}}; L)$ , which is allowed, by the uniqueness, if and only if  $|\Psi_{\text{g.s.}}(\Lambda_{\text{tot}})\rangle \propto \mathcal{P}_{\text{ferro}}(\Lambda_{\text{tot}})|\Psi_{\text{g.s.}}(\Lambda_{\text{tot}})\rangle$ , i.e., the unique ground state is ferromagnetic. This generalizes the rigorous statement for the  $SU(2)$  model in Ref. [33] to arbitrary  $N$ .

### B. Ferromagnetism in high-density region

#### 1. Peculiarity in 1D

Now let us consider the effective Hamiltonian for  $J_K > 0$  which describes the dynamics of the mobile  $\square$  spins in the background of the Kondo singlets  $\bullet$ . The first-order effective Hamiltonian (43a) and (43b) in one dimension (1D) [which we denote by  $\mathcal{H}^{(1)}$ ; see Fig. 5(b-2)] has non-positive off-diagonal matrix elements when  $t > 0$ . However, when the open boundary condition is chosen, these off-diagonal elements simply exchange an adjacent pair of a  $\square$ -spin and a Kondo singlet  $\bullet$  without changing the background  $SU(N)$  spin configurations  $\{\alpha_k\}$  [63], and the lowest-order effective Hamiltonian  $\mathcal{H}^{(1)}$  does not stabilize any particular magnetic orders, as is well-known in the one-dimensional Hubbard model at  $U = \infty$  [64, 65]. Nevertheless, the effective Hamiltonian  $\mathcal{H}^{(1)}$  partially resolves the positional degeneracy thereby reducing the degree of degeneracy  $\binom{L}{\mathcal{N}_{\square}} \times N^{\mathcal{N}_{\square}}$  [with  $\mathcal{N}_{\square} = \mathcal{N}_c - (N - 1)L$  being the number of  $\square$ -spins] down to  $N^{\mathcal{N}_{\square}}$ ; the full  $\mathcal{H}^{(1)}$  decomposes into  $N^{\mathcal{N}_{\square}}$  identical diagonal blocks each of which describes the hopping of  $\mathcal{N}_{\square}$  non-interacting spinless fermions. By the Perron-Frobenius theorem, the ground state of each block (with a given fixed spin configuration  $\{\alpha_k\}$ ) is unique and constructed by summing up all the possible states with the same sequence  $\{\alpha_k\}$  over the positions of the  $\mathcal{N}_{\square}$  fermions with strictly positive coefficients.

This peculiar situation in one dimension is a natural consequence of the equivalence between the one-dimensional  $SU(N)$  KLM (6) and the one-dimensional  $SU(N)$  Hubbard model:

$$\mathcal{H}_{\text{Hubbard}} = -t_H \sum_i \sum_{\alpha=1}^N \left\{ c_{\alpha,i}^\dagger c_{i+1}^\alpha + \text{H.c.} \right\} + U \sum_i n_i(n_i - 1), \quad (46)$$

which generalizes the known equivalence [66] in  $SU(2)$  to  $SU(N)$ . Specifically, the  $U = \infty$  effective Hamiltonian of the model (46) with  $t_H = t/N$  for filling  $0 \leq f \leq 1/N$

coincides with that of the  $J_K = \infty$  SU( $N$ ) KLM for filling  $1 - 1/N \leq f \leq 1$  [(43a) and (43b)].

The above equivalence still holds with the identification  $t_H = t/N$  even in higher dimensions if we treat the  $\square$ -spins as fermions (see Sec. VB for more details). However, the non-positivity is non-trivial since we now have complicated fermion sign factors in front of  $t$ . These sign factors are under control, e.g., when there is only one hole (i.e.,  $\mathcal{N}_c = N\mathcal{N}_\Lambda - 1$  with  $\mathcal{N}_\Lambda$  being the number of lattice sites). In the Hubbard language, the fermion number  $\mathcal{N}_c^{(\text{KLM})} = N\mathcal{N}_\Lambda - 1$  corresponds to  $\mathcal{N}_c^{(\text{Hubbard})} = \mathcal{N}_\Lambda - 1$ , i.e., one less fermion from  $1/N$ -filling, at which we expect the SU( $N$ ) analog of the Nagaoka's ferromagnetism to occur for  $t_H < 0$  [20, 23] if the lattice structure is properly chosen. Therefore, we can borrow the results in the Hubbard model to show that the ground state of the SU( $N$ ) Kondo lattice model in dimensions greater than 1 is ferromagnetic when there is exactly one hole  $\mathcal{N}_c = N\mathcal{N}_\Lambda - 1$  and the lattice satisfies certain conditions.

## 2. Higher-order corrections

The first-order effective Hamiltonian  $\mathcal{H}^{(1)}$  only resolves the degeneracy in the positions of the  $\square$ -spins leaving the  $N^{\mathcal{N}_\square}$ -fold spin degeneracy intact. To lift the huge SU( $N$ )-spin degeneracy in the  $J_K = \infty$  KLM, we need to go to higher orders in  $t$ . We follow the strategy of Ref. [36] and consider the second-order effective Hamiltonian within the (smaller) subspace consisting of the ground states of the first-order Hamiltonian  $\mathcal{H}^{(1)}$ .

We begin with the second-order processes involving two neighboring sites (see Fig. 8). It is easy to see that these  $t^2$  corrections are all diagonal:

$$|N, \alpha\rangle_i \otimes |N, b\rangle_{i+1} \longrightarrow 0 \quad (47a)$$

$$|N, \alpha\rangle_i \otimes |\bullet\rangle_{i+1} \longrightarrow -\left(1 - \frac{1}{N^2}\right) \frac{t^2}{NJ_K} |N, \alpha\rangle_i \otimes |\bullet\rangle_{i+1} \quad (47b)$$

$$|\bullet\rangle_i \otimes |\bullet\rangle_{i+1} \longrightarrow -\frac{N-1}{N+1} \frac{2t^2}{NJ_K} |\bullet\rangle_i \otimes |\bullet\rangle_{i+1}, \quad (47c)$$

from which we can read off the effective interactions:

$$\begin{aligned} & \frac{2(N-1)(2N+1)t^2}{(N+1)N^3J_K} \sum_i n_i(\square)n_{i+1}(\square) \\ & + \frac{2(N-1)(N^2-2N-1)t^2}{(N+1)N^3J_K} \sum_i \left\{ n_i(\square) - \frac{N^2}{N^2-2N-1} \right\} \end{aligned} \quad (48)$$

with  $n_i(\square) = 1$  ( $= 0$ ) when the site  $i$  is occupied by  $\square$  ( $\bullet$ ). Therefore, to find off-diagonal processes, we need to consider three-site processes.

At the order of  $t^2$ , only two types of three-site processes are

possible (see Fig. 9):

$$(i) \quad \begin{array}{c} N-1 \\ \bullet \end{array} - \begin{array}{c} N \\ \square \end{array} - \begin{array}{c} N \\ \square \end{array} \xrightarrow{t} \begin{array}{c} N \\ \square \end{array} - \begin{array}{c} N-1 \\ \square \end{array} \begin{array}{c} \square \\ \square \\ \square \end{array} (\text{adj.}) - \begin{array}{c} N \\ \square \end{array} \quad (49a)$$

$$\begin{aligned} & \xrightarrow{t} \begin{array}{c} N \\ \square \end{array} - \begin{array}{c} N \\ \square \end{array} - \begin{array}{c} N-1 \\ \bullet \end{array} \quad (\Delta E = NJ_K), \\ (ii) \quad \begin{array}{c} N-1 \\ \bullet \end{array} - \begin{array}{c} N-1 \\ \bullet \end{array} - \begin{array}{c} N \\ \square \end{array} \xrightarrow{t} \begin{array}{c} N \\ \square \end{array} - \begin{array}{c} N-2 \\ \square \end{array} \begin{array}{c} \square \\ \square \end{array} (\overline{N}) - \begin{array}{c} N \\ \square \end{array} \quad (49b) \\ & \xrightarrow{t} \begin{array}{c} N \\ \square \end{array} - \begin{array}{c} N-1 \\ \bullet \end{array} - \begin{array}{c} N-1 \\ \bullet \end{array} \quad [\Delta E = (N+1)J_K]. \end{aligned}$$

The corresponding matrix elements read as:

$$(i) \quad |\bullet, N_\alpha, N_\beta\rangle \longrightarrow -\frac{t^2}{N^2J_K} |N_\beta, N_\alpha, \bullet\rangle + \frac{t^2}{N^3J_K} |N_\alpha, N_\beta, \bullet\rangle \quad (50a)$$

$$(ii) \quad |\bullet, \bullet, N_\alpha\rangle \longrightarrow \frac{N-1}{N^2(N+1)J_K} t^2 |N_\alpha, \bullet, \bullet\rangle, \quad (50b)$$

where  $N_\alpha$  is the short-hand notation for  $|N; \alpha\rangle$ . In the first term in (50a), a Kondo singlet  $\bullet$  and  $N_\beta$  interchange their positions with the help of  $N_\alpha$  sitting in the middle [Fig. 9(a)], while in the second, a Kondo singlet  $\bullet$  just goes through  $N_\alpha$  and  $N_\beta$  without disturbing the spin configurations. Obviously, the type-(ii) processes (50b) do not change the spin configurations [Fig. 9(b)].

Now we are at the place of constructing the (spin-only) effective Hamiltonian for the  $N^{\mathcal{N}_\square}$ -dimensional subspace of the spin-degenerate ground states. Let us evaluate the matrix elements of the first term in (50a) that changes the spin configurations. Using the properties of the ground states (of  $\mathcal{H}_1$ ) mentioned in Sec. IV B 1, we readily see that the off-diagonal matrix elements of the second-order Hamiltonian are all non-positive, which allows us to apply the Perron-Frobenius theorem again to prove that the ground state of the Kondo lattice model (6) for sufficiently large  $J_K(> 0)$  is ferromagnetic when  $t > 0$ .

## C. Effects of residual interactions

A few remarks are in order about the effects of several terms that existed in the original two-orbital model (1) but are not explicitly taken into account in the KLM Hamiltonian (6). First, we note that what is crucial to the proof of ferromagnetism is the non-positivity of the off-diagonal matrix elements. Therefore, the conclusion does not change even if we add any kind of diagonal terms (e.g., a non-uniform on-site potential associated with the harmonic trap) as far as they do not conflict with the prerequisites of the strong-coupling expansion.

Also, in deriving the SU( $N$ ) KLM (6) in Sec. II A, we have tentatively dropped the Hubbard  $U^{(g)}$  interaction among the itinerant  $g$ -fermions

$$U^{(g)} n_i(n_i - 1)/2$$

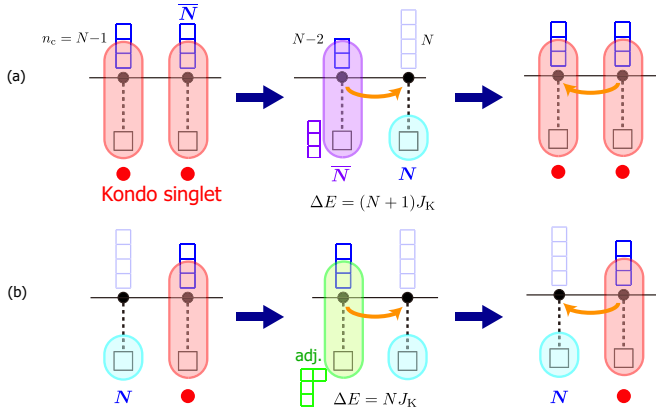


FIG. 8. Two types of second-order processes occurring on a two-site pair  $\bullet-\bullet$  or  $N-\bullet$ . For the  $N-N$  pair, second-order processes are forbidden. The results can be compactly written as a two-body interaction (48).

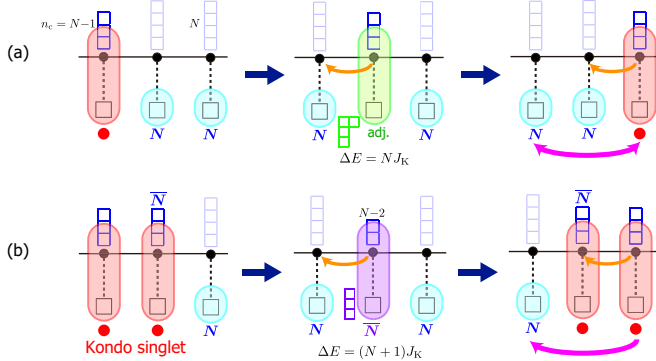


FIG. 9. Second-order processes occurring on three consecutive sites. In the first type, the Kondo singlet moves to the next-nearest-neighbor (NNN) site with the help of the fermion in the middle site. This type of hopping includes (a) the 3-site processes that can change the spin states of the two  $N$ s involved [see (50a)] and (b) those moving the Kondo singlet without changing the background spin configurations [Eq. (50b)]. The second type is just NNN (correlated) hopping of  $N$ .

which may modify the effective Hamiltonians derived in Secs. III B and III C. When  $-J_K (> 0)$  is large enough and  $0 \leq f \leq 1/N$ , we may keep only the  $n_i = 0, 1$  states in which the Hubbard interaction is identically zero. When  $J_K$  is antiferromagnetically large and  $1 - 1/N \leq f \leq 1$ , only the states with  $n_i = N - 1$  and  $N$  are retained. Even in this case, we see that the Hubbard- $U^{(g)}$  is totally irrelevant if we note:

$$\begin{aligned} & \frac{1}{2}U^{(g)}n_i(n_i - 1) \\ &= \frac{1}{2}U^{(g)}\{n_i - (N - 1)\}(n_i - N) + (N - 1)U^{(g)}n_i \\ & - \frac{1}{2}(N - 1)NU^{(g)}. \end{aligned} \quad (51)$$

Therefore, we may conclude that none of the residual terms

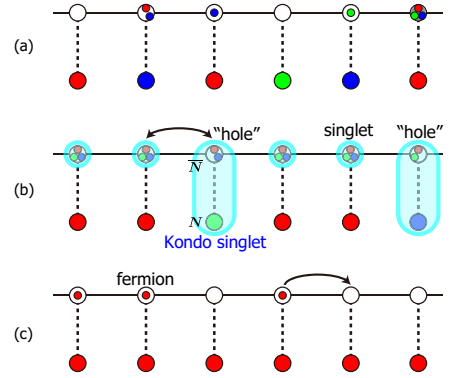


FIG. 10. Ferromagnetic ground states established here (for  $N = 3$ ). (a) A generic configuration and (b) the ferromagnetic ground state for  $J_K > 0$ . For the total “hole” number  $0 \leq \mathcal{N}_h \leq L$  ( $\mathcal{N}_h = NL - \mathcal{N}_c$ ), the same number of the local spins are quenched by forming the Kondo singlets and only the surviving  $L - \mathcal{N}_h$  unquenched moments (colored in red) form the ferromagnetic state. (c) Ferromagnetic ground state for  $J_K < 0$  and total fermion number  $\mathcal{N}_c$  ( $0 \leq \mathcal{N}_c \leq L$ ), in which both  $\mathcal{N}_c$  itinerant and  $L$  local spins participate in ferromagnetism.

in (1) destabilizes the  $SU(N)$  ferromagnetic phases found above. Of course, when these terms are comparable to or larger than the Kondo coupling  $J_K$  which is assumed to be the dominant energy scale here, we expect other phases, e.g., conventional density-wave phases and more exotic symmetry-protected topological phases, to be stabilized [6, 67].

#### D. $SU(N)$ double exchange

In the previous sections, we have rigorously shown that the strong-coupling ground state of the  $SU(N)$  KLM is ferromagnetic in certain regions of the phase diagram. To understand its mechanism simply, we try to generalize the double-exchange mechanism of ferromagnetism put forward in Refs. [30–32] to  $SU(N)$  fermion systems. In order to treat both the itinerant fermions and the local spins within the same framework, we regain the orbital indices  $m = g, e$  ( $g$  for the itinerant fermions and  $e$  for the local spins) used in Sec. II A. We start from the “fully-polarized” state of a local moment (i.e., an immobile  $e$  fermion):

$$|\psi_0\rangle_{S,i} = c_{e1,i}^\dagger |0\rangle_S = |1\rangle_{S,i} \quad (52)$$

which is the  $SU(N)$  analog of  $|\uparrow\rangle$  in  $SU(2)$ . In fact, the above reference state is invariant under the  $U(1) \times U(N - 1)$  (stabilizer) subgroup of  $U(N)$  of the form:

$$\begin{pmatrix} e^{i\theta} & 0 \\ 0 & U(N - 1) \end{pmatrix}.$$

Therefore, only a subset of  $U(N)$  that are parametrized by an  $(N-1)$ -dimensional complex row vector  $\mathbf{q}$  as:

$$\begin{aligned}\widehat{U}(\mathbf{q}) &= \exp[-i\widehat{M}(\mathbf{q})], \\ \widehat{M}(\mathbf{q}) &= (c_{e1}^\dagger, \dots, c_{eN}^\dagger) \left( \begin{array}{c|c} 0 & \mathbf{q} \\ \hline \mathbf{q}^\dagger & \mathbf{0}_{N-1} \end{array} \right) \begin{pmatrix} c_{e1} \\ \vdots \\ c_{eN} \end{pmatrix} \quad (53)\end{aligned}$$

changes the reference state. Roughly, the  $(N-1)$ -dimensional vector  $\mathbf{q}$  plays the same role as the unit vector  $\boldsymbol{\Omega}$  (or the azimuthal and polar angles) in the Bloch coherent state. The fermion operators in the “rotated” frame are:

$$\begin{aligned}\bar{c}_{m\alpha}^\dagger(\mathbf{q}) &= \widehat{U}(\mathbf{q})c_{m\alpha}^\dagger\widehat{U}^\dagger(\mathbf{q}) = \sum_{\beta=1}^N c_{m\beta}^\dagger [U(\mathbf{q})]_{\beta\alpha} \\ \bar{c}_{m\alpha}(\mathbf{q}) &= \widehat{U}(\mathbf{q})c_{m\alpha}\widehat{U}^\dagger(\mathbf{q}) = \sum_{\beta=1}^N [U^\dagger(\mathbf{q})]_{\alpha\beta} c_{m\beta} \quad (m = g, e)\end{aligned} \quad (54)$$

with the  $N \times N$  unitary  $U(\mathbf{q})$  given by

$$U(\mathbf{q}) = \exp \left[ -i \left( \begin{array}{c|c} 0 & \mathbf{q} \\ \hline \mathbf{q}^\dagger & \mathbf{0}_{N-1} \end{array} \right) \right].$$

Using these rotated operators, the coherent state of the local spin at site- $i$  is defined by

$$\begin{aligned}|\mathbf{q}_i\rangle_{S,i} &:= \bar{c}_{e1,i}^\dagger |0\rangle_S = \widehat{U}(\mathbf{q}_i) |\psi_0\rangle_{S,i} \\ &= \sum_{\beta=1}^N [U(\mathbf{q}_i)]_{\beta 1} |\beta\rangle_{S,i} =: \sum_{\beta=1}^N [\mathbf{z}(\mathbf{q}_i)]_{\beta} |\beta\rangle_{S,i}.\end{aligned} \quad (55)$$

The  $N$ -dimensional complex vector  $\mathbf{z}(\mathbf{q}_i)$ , which appeared at the beginning of Sec. IV, is given by the first column vector of  $U(\mathbf{q}_i)$  and satisfies  $|\mathbf{z}(\mathbf{q}_i)| = 1$ . This is the  $SU(N)$ -generalization of the Bloch coherent state

$$|\boldsymbol{\Omega}_i\rangle = e^{-i\frac{\chi_i}{2}} \left\{ e^{-i\frac{\phi_i}{2}} \cos \frac{\theta_i}{2} |\uparrow\rangle + e^{+i\frac{\phi_i}{2}} \sin \frac{\theta_i}{2} |\downarrow\rangle \right\}$$

in which the role of the reference state  $|\psi_0\rangle$  is played by  $|\uparrow\rangle$ . Instead of the vector spin  $\boldsymbol{\Omega}_i(\phi_i, \theta_i)$ , we use the complex unit vector  $\mathbf{z}(\mathbf{q}_i)$  to specify the state  $|\mathbf{q}_i\rangle_{S,i}$  of the local  $SU(N)$  moment at site- $i$ . In the semi-classical approximation, we treat the complex vector  $\mathbf{z}(\mathbf{q}_i)$  as the classical variable which we can fix at will like the classical vector spin. Specifically, we approximate the local (quantum)  $SU(N)$  spins  $S_i^A$  by a set of  $c$ -numbers

$$S^A(\mathbf{q}_i) = \langle \mathbf{q}_i | S_i^A | \mathbf{q}_i \rangle = \mathbf{z}^\dagger(\mathbf{q}_i) G^A \mathbf{z}(\mathbf{q}_i) \quad (56)$$

[with  $G^A$  being the  $N \times N$   $SU(N)$  generators defined in Sec. II]. The exchange interaction between two such semi-classical spins

$$\sum_A S^A(\mathbf{p}_i) S^A(\mathbf{q}_i) = |\mathbf{z}^*(\mathbf{p}_i) \cdot \mathbf{z}(\mathbf{q}_i)|^2 - 1/N.$$

attains its (exact) maximal value  $(1 - 1/N)$  when  $\mathbf{z}(\mathbf{p}_i) = \mathbf{z}(\mathbf{q}_i)$  up to a phase, i.e., when the two spins are coupled ferromagnetically:  $S^A(\mathbf{p}_i) = S^A(\mathbf{q}_i)$ . Therefore, when  $J_K < 0$ , the strong Kondo coupling forces the itinerant and local spins on the same site to be parallel to each other. For the antiferromagnetic  $J_K (> 0)$ , on the other hand, the Kondo energy is minimized for *any* configurations satisfying  $\mathbf{z}^*(\text{itinerant}) \cdot \mathbf{z}(\text{local}) = 0$ . This implies that when  $N \geq 3$ , the direction of the itinerant spin is not determined even if we fix the local moment.

Now let us consider the hopping term. To this end, working with the itinerant ( $g$ ) fermion in the same  $\mathbf{q}$ -frame as the local spin is convenient. Clearly, the  $\alpha = 1$  component  $\bar{c}_{g1,i}$  of the rotated fermions corresponds to the direction of the local spin  $S^A(\mathbf{q}_i)$ . With the help of Eq. (54), we can express the original hopping term by the rotated fermions  $\bar{c}_{g\alpha,i}(\mathbf{q}_i)$ , and the resulting expression contains all the possible hopping processes (including the off-diagonal ones)  $\bar{c}_{g\alpha,i}^\dagger \bar{c}_{g\beta,i+1}$  with the matrix elements

$$-t [U^\dagger(\mathbf{q}_i) U(\mathbf{q}_{i+1})]_{\alpha\beta}.$$

The effect of the strong ferromagnetic Kondo coupling is taken into account by keeping only the  $\alpha = \beta = 1$  component which is “parallel” to the local spin [68]:

$$-t \sum_i \left\{ [\mathbf{z}^\dagger(\mathbf{q}_i) \cdot \mathbf{z}(\mathbf{q}_{i+1})] \bar{c}_{g1,i}^\dagger \bar{c}_{g1,i+1} + \text{H.c.} \right\}. \quad (57)$$

The matrix element can also be written as the overlap  $\langle \mathbf{q}_i | \mathbf{q}_{i+1} \rangle_S$  between the local-spin states (55) on the neighboring sites. Clearly, the hopping amplitude  $|\mathbf{z}^\dagger(\mathbf{q}_i) \cdot \mathbf{z}(\mathbf{q}_{i+1})|$  of the fermions parallel to the local  $SU(N)$  spin  $S^A(\mathbf{q}_i)$  is optimized when  $\mathbf{z}(\mathbf{q}_{i+1}) = \mathbf{z}(\mathbf{q}_i)$  up to a phase, i.e., when the system is ferromagnetic:  $S^A(\mathbf{q}_i) = S^A(\mathbf{q}_{i+1})$  [see Fig. 7(b)]. This is the generalization of the double-exchange mechanism of ferromagnetism in Refs. [30–32] to  $SU(N)$ . Our proof for  $J_K < 0$  tells that this simple argument can be made rigorous in one dimension without relying on the semi-classical approximation.

Difference between  $SU(N = 2)$  and  $SU(N \geq 3)$  becomes manifest in the antiferromagnetic case  $J_K > 0$ . In fact, when  $N = 2$ , we can easily generalize the above mechanism to the case of antiferromagnetic  $J_K$  by keeping itinerant fermions *anti-parallel* to the local moments. However, as strong  $J_K$  alone no longer fixes the relative direction between the itinerant fermion and the local moment for  $N \geq 3$ , the simple double-exchange scenario breaks down when  $J_K > 0$ . Nevertheless, ferromagnetism occurs in the large- $J_K (> 0)$   $SU(N)$  KLM as we have shown rigorously in Sec. IV B.

## V. SUPERSYMMETRY

In Sec. III, we have seen that the strong-coupling effective Hamiltonian contains two local degrees of freedom: two types of mobile spins  $\square$  and  $\square\square$  when  $J_K < 0$ , or  $\bullet$  and  $\square$  when  $J_K > 0$  [see Figs. 5(a-2) and (b-2)]. In the case of  $J_K > 0$ , for instance, each site can take two different  $SU(N)$



states  $\bullet$  (which may be viewed as a hole) and  $\square$  (a particle). As has been mentioned there, the creation and annihilation operators associated with these two (particle and hole) states no longer obey the standard anti-commutation relations for fermions [see Eq. (41)]. The situation is more involved when  $J_K < 0$  as is expected from Eq. (32). Nevertheless, we can regard these mobile spins as a kind of fermionic particles, and the boson-fermion supersymmetry  $SU(N|1)$  provides us with a convenient framework to handle these particles in a unifying way [a quick summary of the super Lie algebra  $SU(N|1)$  is given in Appendix D].

### A. Supersymmetric $SU(N)$ $t$ - $J$ model

The super Lie algebra  $SU(N|1)$  consists of  $N^2$  bosonic [see Eq. (D1)] and  $2N$  fermionic [Eq. (D2)] generators satisfying particular algebraic relations (D4a)–(D4d). The state vector of the simplest  $(N+1)$ -dimensional irreducible representation decomposes into two parts; the first  $N$  components and the last one of the state vectors correspond to two different  $SU(N)$  representations  $N$  ( $\square$ ) and the singlet ( $\bullet$ ), respectively [see Eq. (D1)]. The  $N^2$  bosonic generators are all block-diagonal with respect to these two sectors, while the  $2N$  fermionic ones bring about the transitions between them.

The simplest  $SU(N|1)$ -symmetric interaction can be found by considering the quadratic Casimir (D6) which is a super-Lie-algebraic analog of  $S^2$  in  $SU(2)$ :

$$C_2 = \sum_{A=1}^{N^2-1} \mathcal{S}^A \mathcal{S}^A - \frac{1}{N(N-1)} \mathcal{K}^2 - \sum_{\alpha=1}^N \left( \mathcal{Q}_\alpha \tilde{\mathcal{Q}}_\alpha - \tilde{\mathcal{Q}}_\alpha \mathcal{Q}_\alpha \right)$$

with the bosonic generators  $\mathcal{X} = \mathcal{S}^A, \mathcal{K}$  ( $A = 1, \dots, N^2 - 1$ ) and the fermionic ones  $\mathcal{X} = \mathcal{Q}_\alpha, \tilde{\mathcal{Q}}_\alpha$  ( $\alpha = 1, \dots, N$ ) given respectively by Eqs. (D1) and (D2). Then, it is straightforward to write the  $SU(N|1)$ -symmetric interaction as:

$$\begin{aligned} C_2(\mathcal{X}_i + \mathcal{X}_j) &= C_2(\mathcal{X}_i) + C_2(\mathcal{X}_j) - 2 \sum_{\alpha=1}^N \left( \mathcal{Q}_{\alpha,i} \tilde{\mathcal{Q}}_{\alpha,j} - \tilde{\mathcal{Q}}_{\alpha,i} \mathcal{Q}_{\alpha,j} \right) \\ &\quad + 2 \left\{ \sum_{A=1}^{N^2-1} \mathcal{S}_i^A \mathcal{S}_j^A - \frac{1}{N(N-1)} \mathcal{K}_i \mathcal{K}_j \right\} \end{aligned} \quad (58)$$

where the constant  $C_2(\mathcal{X}) = \frac{N(N-2)}{N-1}$ . Depending both on the irreducible representation we use and on how the local degrees of freedom realize in specific physical systems, the Hamiltonian (58) describes different physical situations. For instance, if we use the simplest  $(N+1)$ -dimensional representation and identify the first  $N$  and the last one components as describing a fermionic particle carrying the  $SU(N)$ -spin  $\square$  and a hole, respectively,  $\mathcal{Q}_\alpha, (\tilde{\mathcal{Q}}_\alpha)$  creates (annihilates) the  $\square$ -particle; the term  $\mathcal{Q}_{\alpha,i} \tilde{\mathcal{Q}}_{\alpha,j} - \tilde{\mathcal{Q}}_{\alpha,i} \mathcal{Q}_{\alpha,j}$  simply expresses the hopping of the  $\square$ -spin, and the model (58) describes interacting (fermionic)  $\square$ -particles hopping in the background

of holes ( $\bullet$ ). Typically, this situation occurs in the  $U = \infty$   $SU(N)$  Hubbard model. In this simplest realization, the model (58) is known as the supersymmetric  $SU(N)$   $t$ - $J$  model [69–71] which is an  $SU(N)$ -generalization of the usual supersymmetric  $t$ - $J$  model for  $N = 2$  [72, 73]. Thanks to the exact solution, low-energy physics is well understood and is known to be described by the  $N$ -component  $U(1) \times SU(N)_1$  Tomonaga-Luttinger liquid [70].

### B. Antiferromagnetic Kondo coupling

To realize a supersymmetric model in the strong-coupling limit of the antiferromagnetic  $SU(N)$  KLM, we first need to identify the projected fermion operators  $\tilde{c}_{\alpha,i}^\dagger$  and  $\tilde{c}_i^\alpha$  (40) with the fermionic generators (D2) of  $SU(N|1)$ . The idea is to combine the  $N$  states ( $|N; \alpha\rangle$ ) with a  $\square$ -spin occupying the site and the Kondo singlet ( $|\bullet\rangle$ ) into a single  $(N+1)$ -component multiplet. Looking at the structure of the  $SU(N|1)$  representation (D9), we see that the  $n = 1$  case of the F-B construction (D7a)–(D7b) works. Specifically, we identify the states  $|N; \alpha\rangle$  and the Kondo singlet  $|\bullet\rangle$  with the states with the boson-fermion occupation  $(n_F, n_B) = (1, 0)$  and  $(n_F, n_B) = (0, 1)$ , respectively (see Table II; this seems quite natural from the original spirit of the slave-boson construction [74]). The commutation relations (D4c) suggest us to identify

$$\mathcal{Q}_\alpha \leftrightarrow \tilde{c}_\alpha^\dagger, \quad \tilde{\mathcal{Q}}_\alpha \leftrightarrow \tilde{c}^\alpha \quad (\alpha = 1, \dots, N)$$

up to an overall factor. If we assign the states  $|N; \alpha\rangle$  ( $\alpha = 1, \dots, N$ ) to the first  $N$  components, and the Kondo singlet  $|\bullet\rangle$  to the  $(N+1)$ -th component [note that the  $SU(N)$ -singlet  $|\bullet\rangle$  here is not necessarily the same as the *physical* Kondo singlet  $|\bullet'\rangle$ ], the anti-commutator (D4b) reads as [use (D5)]:

$$\{\mathcal{Q}_\alpha, \tilde{\mathcal{Q}}_\beta\} = |N; \alpha\rangle \langle N; \beta| + \delta_{\alpha\beta} |\bullet\rangle \langle \bullet|. \quad (59)$$

If we identify the many-body basis states

$$|\dots\rangle \otimes |N; \alpha_{i_1}\rangle_{i_1} \otimes |\dots\rangle \otimes |N; \alpha_{i_2}\rangle_{i_2} \otimes \dots$$

(where  $|\dots\rangle$  stands for the product of the physical Kondo singlets  $|\bullet'_i\rangle$  in Eqs. (43a), (43b), and (44) with the states

$$\mathcal{Q}_{\alpha_{i_1}, i_1} \mathcal{Q}_{\alpha_{i_2}, i_2} \dots |\bullet\rangle^{\otimes L},$$

all the sign factors arising from the anti-commutation of the original fermions  $c_{\alpha,i}^\dagger$  and  $c_i^\alpha$  are taken into account by that of  $\mathcal{Q}_{\alpha,i}$  and  $\tilde{\mathcal{Q}}_{\alpha,i}$  on different sites. With this identification, we see that the fermionic generators  $\{\mathcal{Q}_{\alpha,i}, \tilde{\mathcal{Q}}_{\alpha,i}\}$  are related to the projected fermion operators as:

$$\mathcal{Q}_{\alpha,i} = (-1)^{N-1} \sqrt{N} \tilde{c}_{\alpha,i}^\dagger, \quad \tilde{\mathcal{Q}}_{\alpha,i} = (-1)^{N-1} \sqrt{N} \tilde{c}_i^\alpha, \quad (60)$$

which correctly reproduces (41) from (59). The bosonic generator  $\mathcal{K}_i$  essentially counts the number of the Kondo singlets at site- $i$  [multiplied by a factor  $(N-1)$ ] which physically corresponds to that of holes:

$$\begin{aligned} \mathcal{K}_i &= 1 + (N-1) |\bullet\rangle \langle \bullet|_i = 1 + (N-1)(N - \tilde{n}_i) \\ &= (N^2 - N + 1) - (N-1)\tilde{n}_i \quad (\tilde{n}_i = N-1, N). \end{aligned} \quad (61)$$



The bosonic  $SU(N)$  spin operators  $S^A$  are given in Eq. (D1).

Using the relations (60) and (61), we see that the following effective Hamiltonian at the special point  $\mathcal{J} = t/N$  is  $SU(N|1)$ -symmetric:

$$\begin{aligned} \mathcal{H}_{\text{SUSY}}^{(\text{AF})} = & -t \sum_i \sum_{\alpha=1}^N \left( \tilde{c}_{\alpha,i}^\dagger \tilde{c}_{\alpha,i+1} + \tilde{c}_{\alpha,i+1}^\dagger \tilde{c}_{\alpha,i} \right) \\ & + \mathcal{J} \sum_i \left\{ \sum_{A=1}^{N^2-1} S_i^A S_{i+1}^A - \frac{N-1}{N} \tilde{n}_i \tilde{n}_{i+1} \right\} \quad (62) \\ & + \frac{2(N^2 - N + 1)}{N^2} t \sum_i \tilde{n}_i + \text{const.} \end{aligned}$$

The two terms in the second line do not exist in the effective Hamiltonian of the usual  $SU(N)$  KLM (6). In fact, the local  $SU(N)$  spin  $S^A$  projected onto the ground-state subspace spanned by the states (38a) and (38b) is either 0 (when the site is occupied by the Kondo singlet) or  $S^A(\square) = G^A$  (when the site is in  $\square$ ). This perfectly fits the form of the  $SU(N|1)$  generators  $S^A$  in Eq. (D1):

$$S^A \xrightarrow{\text{proj.}} \tilde{S}^A = \left( \begin{array}{c|c} S^A(\square) & 0 \\ \hline 0 & 0 \end{array} \right) = S^A. \quad (63)$$

Therefore, the first term is obtained just by projecting the Heisenberg interaction among the local spins:

$$J_H S_i^A S_j^A \xrightarrow{\text{proj.}} J_H \tilde{S}_i^A \tilde{S}_j^A.$$

The second is provided by an attractive interaction between the fermions at sites  $i$  and  $j$ . Summarizing all these, we conclude that the supersymmetric interaction (62) is obtained in the  $J_K = \infty$  limit of the (generalized) Kondo-Heisenberg model (8):

$$\begin{aligned} \mathcal{H}_{\text{KHM}} = & -t \sum_i \sum_{\alpha=1}^N \left( c_{\alpha,i}^\dagger c_{\alpha,i+1} + \text{h.c.} \right) + J_K \sum_i \left( \sum_{A=1}^{N^2-1} \hat{s}_i^A S_i^A \right) \\ & + J_H \sum_i \left( \sum_{A=1}^{N^2-1} S_i^A S_{i+1}^A \right) + V \sum_i n_i n_{i+1} \end{aligned}$$

with

$$J_H = \frac{t}{N}, \quad V = -\frac{N-1}{N^2} t. \quad (64)$$

A few remarks are in order about the supersymmetric point. By construction, it is obvious that the supersymmetric interaction (58) is defined with respect, not to the physical operators (e.g.,  $c_{\alpha,i}^\dagger, c_{\alpha,i}$ ) but to the supersymmetry (SUSY) generators  $\{S^A, \mathcal{K}, \mathcal{Q}, \tilde{\mathcal{Q}}\}$ . Therefore, depending on how we identify the  $SU(N|1)$  generators with the physical operators (and how we define the local degrees of freedom), the resulting supersymmetric models may be different. For instance, if we realize the

$SU(N)$   $t$ - $J$  model (62) in the large- $U$  limit of the  $SU(N)$  Hubbard model in which multiply-occupied sites are projected out, we have different relations  $\mathcal{Q}_\alpha = \tilde{c}_\alpha^\dagger$  and  $\tilde{\mathcal{Q}}_\alpha = \tilde{c}_\alpha$  instead of (60). Plugging these into Eq. (58), we see that now  $\mathcal{J} = t$  corresponds to the supersymmetric point [75]. On the other hand, the exchange interaction is given by  $\mathcal{J} = 2t^2/U$  which must be much smaller than  $t$ . In this sense, the supersymmetric model (derived from the large- $U$  Hubbard model) with  $\mathcal{J} = t$  seems unrealistic. However, when we use the large- $J_K$  limit of the  $SU(N)$  Kondo-Heisenberg model (8) to realize the same  $SU(N)$   $t$ - $J$  model, the supersymmetric point corresponds to  $\mathcal{J} = J_H = \frac{t}{N} (< t)$ , which seems more feasible.

TABLE II. Interpretation of the  $SU(N)$  and SUSY states in terms of fermionic states. In the ground-state subspace, the projected fermion number  $\tilde{n}$  takes  $N-1$  and  $N$ .

fermionic states	$\tilde{n}$	$SU(N)$ irreps.	$(n_F, n_B)$
$ \mathbf{f}\rangle_{F,i}$	$N$	$ \mathbf{N}; \alpha\rangle_i (\square)$	$(1, 0)$
$ \alpha\rangle_{F,i} = c_i^\alpha  \mathbf{f}\rangle_{F,i}$	$N-1$	$ \bullet\rangle_i$ (Kondo singlet)	$(0, 1)$

### C. Ferromagnetic Kondo coupling

When  $J_K$  is ferromagnetically large, the effective Hamiltonian contains the two types of mobile spins  $\square$  and  $\square$  instead of  $\square$  and the Kondo singlets  $\bullet$  for  $J_K > 0$ . Accordingly, the local  $SU(N)$  spin operators are given either by  $S^A(\square)$  or by  $S^A(\square)$ . To describe these two states on an equal footing, we now use  $SU(N|1)$  in the “B-F” (or, slave-fermion) construction (D10a) and (D10b) with the total particle number  $n = n_B + n_F = 2$ , in which the boson-fermion occupation  $(n_B, n_F) = (2, 0)$  and  $(n_B, n_F) = (1, 1)$  correspond to the states  $\square$  and  $\square$ , respectively [see Eq. (D12)]. The correspondence among the (projected) fermion number  $\tilde{n}$ , the  $SU(N)$  representations, and the  $SU(N|1)$  states is summarized in Table III.

As in the previous section, we begin with identifying the projected fermion operators (32) with the fermionic generators  $\mathcal{Q}$  and  $\tilde{\mathcal{Q}}$  in the  $n = 2$  representation which is *different* from the one used in the previous section. Using (D13a) and (D13b), we can write the matrix elements of the fermionic generators that create the  $\square$  spin out of  $\square$  as:

$$\begin{aligned} \mathcal{Q}_\alpha = & \sqrt{2} |(\alpha, \alpha)\rangle \langle \mathbf{N}; \alpha| \\ & + \sum_{\beta > \alpha} |(\alpha, \beta)\rangle \langle \mathbf{N}; \beta| + \sum_{\beta < \alpha} |(\beta, \alpha)\rangle \langle \mathbf{N}; \beta| \quad (65) \\ = & \tilde{\mathcal{Q}}_\alpha^\dagger, \end{aligned}$$

which immediately enables us to identify:

$$\mathcal{Q}_{\alpha,i} = \sqrt{2} \tilde{c}_{\alpha,i}^\dagger, \quad \tilde{\mathcal{Q}}_{\alpha,i} = \sqrt{2} \tilde{c}_i^\alpha. \quad (66a)$$

This is natural since  $c_{\alpha,i}^\dagger$  ( $c_i^\alpha$ ) creates (annihilates) the  $\square$ -particles. The two bosonic generators are now given in terms

of the physical operators by:

$$\mathcal{S}_i^A = \left( \begin{array}{c|c} S_i^A(\square\square) & 0 \\ \hline 0 & S_i^A(\square) \end{array} \right) \quad (66b)$$

[with  $S_i^A(\square\square)$  being the  $SU(N)$  generator in the  $[N(N+1)/2]$ -dimensional representation  $\square\square$ ] and

$$\mathcal{K}_i = n_B + Nn_F = (N+1) - (N-1)\tilde{n}_i \\ = \left( \begin{array}{c|c} 2 \times \mathbf{1}_{N(N+1)/2} & 0 \\ \hline 0 & (N+1) \times \mathbf{1}_N \end{array} \right) \quad (66c)$$

where we have used  $n_B + n_F = 2$  and  $n_B = \tilde{n}_i + 1$  (with the local  $c$ -fermion number  $\tilde{n}_i = 0, 1$ ). Out of these generators, we can readily construct the supersymmetric Hamiltonian (58):

$$\mathcal{H}_{\text{SUSY}}^{(\text{FM})} = -t \sum_i \sum_{\alpha=1}^N \left( \tilde{c}_{\alpha,i}^\dagger \tilde{c}_{\alpha,i+1}^\alpha + \tilde{c}_{\alpha,i+1}^\dagger \tilde{c}_i^\alpha \right) \\ + \mathcal{J} \sum_i \left\{ \sum_{A=1}^{N^2-1} \mathcal{S}_i^A \mathcal{S}_{i+1}^A - \frac{N-1}{N} \tilde{n}_i \tilde{n}_{i+1} \right\} \quad (67) \\ + \frac{N+1}{N} t \sum_i \tilde{n}_i + \text{const.}$$

with  $\mathcal{J} = t/2$ . This looks the same as (62) except that now the particles created or annihilated by  $\tilde{c}_{\alpha,i}^\dagger$  and  $\tilde{c}_i^\alpha$  are  $\square\square$  spins embedded in the  $\square$  background [see Fig. 5(a-2)]. Correspondingly, the supersymmetric point *in the physical model* is shifted:  $\mathcal{J} = t/N$  (AF)  $\rightarrow t/2$  (FM). Interestingly, the two supersymmetric models (62) and (67) emerge from the same Kondo-Heisenberg model depending on the sign of  $J_K$  and filling ( $f = 1/N$  or  $1 - 1/N$ ).

The origin of the interactions other than the spin exchange is obvious. One may think that, as in the antiferromagnetic case, the spin exchange  $\mathcal{S}_i^A \mathcal{S}_{i+1}^A$  comes from the spin-spin interaction ( $J_H$ ) among the local spins. However, as the local  $SU(N)$  spin  $S^A$  acts differently on the two local degrees of freedom ( $\square\square$  and  $\square$ ), its projected expression is now given by [see Eq. (63)]:

$$\tilde{S}_i^A = \left( \begin{array}{c|c} \frac{1}{2} S_i^A(\square\square) & 0 \\ \hline 0 & S_i^A(\square) \end{array} \right) \quad (68)$$

which is different from the generator  $\mathcal{S}_i^A$  appearing in (67) [see Eq. (66b) for the definition of  $\mathcal{S}_i^A$ ]. Therefore, to realize the supersymmetric interaction, we need to slightly modify the  $J_H$  interaction in the Kondo-Heisenberg model (8) in such a way that it includes diagonal (i.e. off-site) Kondo couplings as well:

$$J_H \sum_i \left( \sum_{A=1}^{N^2-1} \mathcal{S}_i^A \mathcal{S}_{i+1}^A \right) \\ \rightarrow J_H \sum_i \left\{ \sum_{A=1}^{N^2-1} (\hat{S}_i^A + S_i^A)(\hat{S}_{i+1}^A + S_{i+1}^A) \right\}. \quad (69)$$

Then, setting

$$J_H = \frac{t}{2}, \quad V = -\frac{N-1}{2N}t \quad (70)$$

and  $J_K = -\infty$  in the generalized Kondo-Heisenberg model (8) realizes the supersymmetric model (67).

Unfortunately, the behavior of the “higher-spin”  $SU(N)$   $t$ - $J$  model (67) is not known except at  $\mathcal{J} = 0$  where we have rigorously established in Sec. IV A that the ground state is ferromagnetic. The inclusion of the  $\mathcal{J} (> 0)$ -term that favors antiferromagnetic correlation may destabilize the ferromagnetic ground state as in the  $N = 2$  case [76, 77]. In this sense, the supersymmetric point at which the two tendencies compete might play a special role and the search for the exactly solvable supersymmetric “spin” Hamiltonians [78–80] would be interesting.

TABLE III. Correspondence among fermionic states,  $SU(N)$ -spin, and SUSY representation

fermionic states	$\tilde{n}$	$SU(N)$ spin states	$(n_B, n_F)$
$ \alpha\rangle_{F,i} = c_{\alpha,i}^\dagger  0\rangle_{F,i}$	1	$ (\alpha, \beta)\rangle_i(\square\square)$	(2, 0)
$ 0\rangle_{F,i}$	0	$ \mathbf{N}; \alpha\rangle_i(\square)$	(1, 1)

## VI. SUMMARY AND DISCUSSION

In this paper, we have considered the ground state of the  $SU(N)$  Kondo lattice model with the local spins in the  $N$ -dimensional defining representation ( $\square$ ) for sufficiently strong Kondo coupling. Specifically, we have shown rigorously that the ground state of the one-dimensional model (with open boundary condition) for fillings  $0 < f < 1/N$  (when  $J_K < 0$ ) and  $1 - 1/N < f < 1$  (when  $J_K > 0$ ) is ferromagnetic. The corresponding ferromagnetic states are shown schematically in Figs. 10(b) and (c). The proof is based on the Perron-Frobenius theorem on the spectral properties of irreducible non-positive matrices. In higher dimensions, we can make a similar statement on ferromagnetism, e.g., when there is precisely one fewer fermion from the commensurate filling  $f = 1/N$  or 1. We can also treat the problem with one fermion or one hole exactly for any  $J_K \neq 0$  (i.e., without relying on the strong-coupling limit) to prove the ferromagnetic ground states. Therefore, in the extreme limits  $f \rightarrow 0$  ( $J_K < 0$ ) and  $f \rightarrow 1$  ( $J_K > 0$ ), the ferromagnetic phases are expected to persist down to  $J_K \rightarrow \pm 0$  (see Fig. 11). For the situation considered in this paper, we can generalize the double-exchange scenario to  $SU(N)$  with due complication, which semi-classically explains the occurrence of ferromagnetism for  $J_K < 0$ . Considering the large positive scattering  $g$ - $e$  length of  $^{173}\text{Yb}$  which suggests a large ferromagnetic  $J_K$ ,  $^{173}\text{Yb}$  would be a promising system to test the  $SU(N)$  double-exchange mechanism in the strongly-coupled KLM.

At the special filling fractions  $f = 1/N$  and  $1 - 1/N$ , the system is insulating. When  $f = 1 - 1/N$  and  $J_K \gg t$ , the system is a spin-gapped insulator, which is the  $SU(N)$ -analog

of the well-known Kondo insulator in the usual SU(2) KLM at half-filling. On the other hand, in the insulating phase at  $f = 1/N$  and  $-J_K \gg t$ , the behavior of the spin sector depends on the parity of  $N$ ; the spin correlation is algebraic (exponentially decaying) when  $N = \text{odd}$  ( $N = \text{even}$ ). The schematic phase diagram that summarizes the main results of this paper is given in Fig. 11.

As has been seen in Sec. III, the low-energy physics at strong coupling is described by two different degrees of freedom [Kondo singlets and mobile  $N$  spins for  $J_K > 0$ , and mobile two species of spins  $N$  ( $\square$ ) and  $\square$  for  $J_K < 0$ ]. We have found that the language of super Lie algebra SU( $N|1$ ) perfectly fits into these situations and can describe the low-energy processes in a natural way. In fact, for particular sets of parameters, we can realize the supersymmetric models in the limit of strong Kondo coupling. The resulting conditions for supersymmetry are milder (or more realistic) than the one known for the  $t$ - $J$  model.

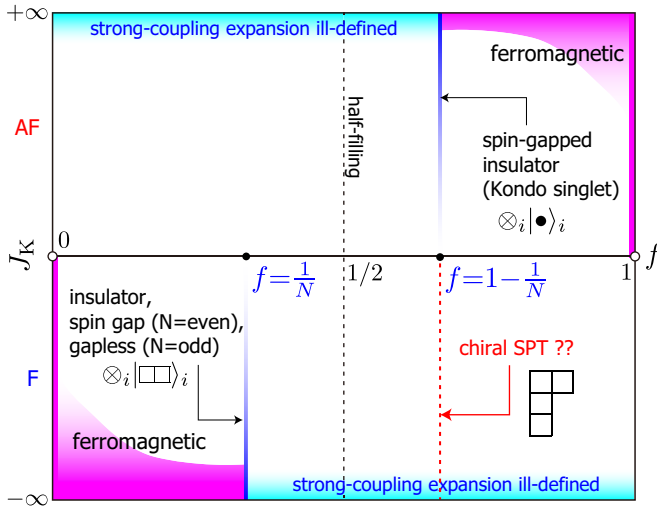


FIG. 11. Strong-coupling phases in SU( $N$ ) Kondo lattice model in 1D. The insulating phase at  $f = 1/N$  ( $J_K < 0$ ) has a finite spin gap only when  $N$  is even, while the one at  $f = 1 - 1/N$  ( $J_K > 0$ ) is fully gapped. The ferromagnetic phases (highlighted in magenta) extend to the lower-density (when  $J_K < 0$ ) or higher-density ( $J_K > 0$ ) side of these insulating phases. At the extreme limits  $f \rightarrow 0$  ( $N_c = 1$ ) or  $f \rightarrow 1$  ( $N_c = NL - 1$ ; one hole), we can establish ferromagnetism regardless of the magnitude of  $J_K$  ( $\neq 0$ ).

## ACKNOWLEDGEMENTS

The authors would like to thank S. Capponi, K. Hasebe, H. Katsura, N. Kawakami, P. Lecheminant, K. Ono, D. Papular, and Y. Takahashi for helpful discussions and correspondences. The author is supported in part by the Japan Society for the Promotion of Science (JSPS) KAKENHI Grant No. 18K03455 and No. 21K03401.

## Appendix A: Young diagrams and SU( $N$ ) representations

In this appendix, we give a quick explanation of what the Young diagrams stand for in physical terms. Let us first introduce the fundamental representations that are building blocks of all possible irreducible representations. There are  $N - 1$  fundamental representations  $\mathcal{R}_n$  each of which is realized by a fixed number  $n$  ( $= 1, \dots, N - 1$ ) of  $N$ -colored fermions  $c_\alpha^\dagger$  ( $\alpha = 1, \dots, N$ ) [the two cases  $n = 0, N$  correspond to SU( $N$ )-singlet and are trivial]. The  $n$ -fermion representation  $\mathcal{R}_n$  is spanned by the states of the form (the bracket  $[\dots]$  stands for anti-symmetrization):

$$|[\alpha_1, \dots, \alpha_n]\rangle := c_{\alpha_1}^\dagger c_{\alpha_2}^\dagger \cdots c_{\alpha_n}^\dagger |0\rangle_F \quad (\text{A1})$$

and has dimensions  $\frac{N!}{(N-n)!n!}$ . If necessary, we can easily calculate the corresponding matrix representation using the second quantized generators similar to (3). We assign the following single-column Young diagrams

$$\mathcal{R}_n : \quad n \left\{ \begin{array}{c} \square \\ \square \\ \vdots \\ \square \end{array} \right\} \quad (n = 1, \dots, N - 1) \quad (\text{A2})$$

to these representations. By construction, the  $n$  boxes in the same column are anti-symmetrized. The simplest of them is the  $N$ -dimensional representation  $\square$  which is spanned by the following  $N$  single-fermion ( $n = 1$ ) states:

$$|\alpha\rangle := c_\alpha^\dagger |0\rangle_F \quad (\alpha = 1, \dots, N)$$

and has been used for the local spins of the models (6) and (8).

The conjugate representation  $\bar{\mathcal{R}}_n$  of  $\mathcal{R}_n$  is obtained by applying the particle-hole transformation:

$$\begin{aligned} |[\alpha_1, \dots, \alpha_n]\rangle &:= c^{\alpha_n} \cdots c^{\alpha_1} |f\rangle_F \\ &= \frac{1}{(N-n)!} \sum_{\{\beta_i\}} \epsilon^{\alpha_1 \cdots \alpha_n \beta_{n+1} \cdots \beta_N} |[\beta_{n+1}, \dots, \beta_N]\rangle \\ &\quad \left( |f\rangle_F = c_1^\dagger \cdots c_N^\dagger |0\rangle_F \right). \end{aligned}$$

As the right-hand side transforms like  $\mathcal{R}_{N-n}$ , the conjugation transforms the Young diagram as:

$$n \left\{ \begin{array}{c} \square \\ \square \\ \vdots \\ \square \end{array} \right\} (\mathcal{R}_n) \xrightarrow{\text{conjugate}} N-n \left\{ \begin{array}{c} \square \\ \square \\ \vdots \\ \square \end{array} \right\} (\bar{\mathcal{R}}_n = \mathcal{R}_{N-n}). \quad (\text{A3})$$

Clearly, the  $N$  one-hole states

$$|\alpha\rangle = c^\alpha |f\rangle_F = (-1)^{\alpha-1} \prod_{\beta \neq \alpha} c_\beta^\dagger |0\rangle_F \quad (\alpha = 1, \dots, N)$$

appearing in Eq. (37) span the conjugate  $\bar{\mathcal{R}}_1$  of the one-fermion representation  $\mathcal{R}_1$  ( $\square$ ).

The generic irreducible representations are constructed by tensoring the  $N - 1$  fundamental representations  $\mathcal{R}_n$ :

$$\mathcal{R}_1^{\otimes d_1} \otimes \cdots \otimes \mathcal{R}_{N-1}^{\otimes d_{N-1}}. \quad (\text{A4})$$

In doing so with fermions, we need to introduce an additional degree of freedom (“flavor”) on top of the color  $\alpha$  (=



From these, the Kondo energy (19) is readily calculated as:

$$e_K = -\frac{N+1}{N}n_c J_K \quad \text{for } n_{c+1} \left\{ \begin{array}{c} \square \\ \square \\ \square \end{array} \right\},$$

$$e_K = \left(1 - \frac{n_c}{N}\right) J_K \quad \text{for } n_c \left\{ \begin{array}{c} \square \\ \square \\ \square \end{array} \right\} \quad (1 \leq n_c \leq N-1)$$

$$e_K = 0 \quad (n_c = 0, N).$$
(B7)

As is shown in Fig. 3, the Kondo energy  $e_K$  is concave at  $n_c = 1$  (when  $J_K < 0$ ) or  $n_c = N-1$  (when  $J_K > 0$ ), and except there it is linear in  $n_c$ .

### Appendix C: Irreducibility of the Hamiltonian

In this appendix, we sketch the proof of the irreducibility of the one-dimensional effective Hamiltonian (33). The proof is based on mathematical induction with respect to the system size  $L (\geq 2)$  [77]. Suppose that the Hamiltonian is irreducible for a system sizes  $L = L_0$ , and for *all* values of  $\mathcal{N}_c$  ( $1 \leq \mathcal{N}_c \leq L_0 - 1$ ) and any total weights  $\Lambda_{\text{tot}}$  allowed for  $L_0$  and  $\mathcal{N}_c$ . Since the Hamiltonian is identically zero when  $\mathcal{N}_c = 0$  (no fermion to move) and when  $\mathcal{N}_c = L_0$  (no hole to move), we must exclude these cases as trivial.

To find the connectivity structure, we group the basis states of the  $(L_0 + 1)$ -site system (with the total  $\text{SU}(N)$  weight  $\Lambda_{\text{tot}}$  and the fermion number  $1 \leq \mathcal{N}_c \leq L_0$ ) according to the states at the site- $(L_0 + 1)$ :

$$(i): |\{\lambda_i\}; \alpha\rangle_{i_1, i_2, \dots, i_{\mathcal{N}_c}} = \left| i_1, i_2, \dots, i_{\mathcal{N}_c}; \{\lambda_i\}_{\sum_{i=1}^{L_0} \lambda_i = \Lambda_{\text{tot}} - \lambda_\alpha} \right\rangle \otimes |\square; \lambda_\alpha\rangle_{L_0+1}$$

$$(\alpha = 1, \dots, N)$$

$$(ii): |\{\lambda_i\}; (\alpha, \beta)\rangle_{i_1, i_2, \dots, i_{\mathcal{N}_c-1}, L_0+1} = \left| i_1, i_2, \dots, i_{\mathcal{N}_c-1}; \{\lambda_i\}_{\sum_{i=1}^{L_0} \lambda_i = \Lambda_{\text{tot}} - \lambda_\alpha - \lambda_\beta} \right\rangle$$

$$\otimes |\square; \tilde{\lambda}_{(\alpha, \beta)}\rangle_{L_0+1} \quad (1 \leq \alpha \leq \beta \leq N),$$
(C1)

where the sequence  $\{i_1, i_2, \dots, i_{\mathcal{N}_c}\}$  specifies the positions of fermions (i.e., those of  $\square$ -spins), and the set of the local  $\text{SU}(N)$  weights  $\{\lambda_i\}$  ( $i = 1, \dots, L_0$ ) satisfies  $\sum_{i=1}^{L_0} \lambda_i + \lambda_{L_0+1} = \Lambda_{\text{tot}}$  ( $\lambda_{L_0+1} = \lambda_\alpha, \tilde{\lambda}_{(\alpha, \beta)}; \tilde{\lambda}_{(\alpha, \beta)} = \lambda_\alpha + \lambda_\beta$ ). In (i), all the  $\mathcal{N}_c$  fermions are contained in the  $L_0$ -site subsystem, while in (ii), one of the fermions is sitting at site- $(L_0 + 1)$ .

When the hopping between the sites  $L_0$  and  $(L_0 + 1)$  is absent, the effective Hamiltonian assumes a block-diagonal form, in which each of the block matrices is irreducible by the assumption except for  $\mathcal{N}_c = 1$  and  $L_0$  [81]. We denote these  $N(N+3)/2$  diagonal blocks by:  $\mathbf{B}_\alpha^\square$  ( $\alpha = 1, \dots, N$ ) and  $\mathbf{B}_{(\alpha, \beta)}^\square$  ( $1 \leq \alpha, \beta \leq N$ ). When the hopping between  $L_0$  and

$(L_0 + 1)$  is switched on, the following transitions are allowed:

$$|\{\lambda_i\}; \alpha\rangle_{i_1, i_2, \dots, i_{\mathcal{N}_c-1}, i_{\mathcal{N}_c} = L_0}$$

$$\rightarrow \sum_{\beta=1}^N |\{\lambda'_i\}; (\alpha, \beta)\rangle_{i_1, i_2, \dots, i_{\mathcal{N}_c-1}, L_0+1}$$

$$[\lambda'_i = \lambda_i \ (i = 1, \dots, L_0 - 1), \lambda'_{L_0} = \lambda_{L_0} - \lambda_\beta]$$

$$|\{\lambda_i\}; (\alpha, \beta)\rangle_{i_1, i_2, \dots, i_{\mathcal{N}_c-1} (< L_0), L_0+1}$$

$$\rightarrow \sum_{\gamma} |\{\lambda'_i\}; \gamma\rangle_{i_1, i_2, \dots, i_{\mathcal{N}_c} = L_0}$$

$$(\gamma = \alpha, \beta \text{ when } \alpha \neq \beta, \gamma = \alpha \text{ when } \alpha = \beta; \sum_{i=1}^{L_0} \lambda'_i = \Lambda_{\text{tot}} - \lambda_\gamma),$$
(C2)

where we have omitted the non-zero numerical coefficients. The new connectivity structure introduced by the hopping between the sites  $L_0$  and  $(L_0 + 1)$  may be best visualized by the graphs shown in Fig. 13. To construct the graph representing the connectivity among the  $N(N+3)/2$  groups of basis states, we first draw a complete graph made of  $N$  vertices (colored in pink)  $\alpha = 1, \dots, N$ , in which each vertex represents one of the type-(i) groups of states in (C1) and is associated with the block matrices  $\mathbf{B}_\alpha^\square$ . By the assumption, all the states contained in the vertex  $\alpha$  are connected to each other by the action of  $\mathbf{B}_\alpha^\square$ . Then, on the edges  $(\alpha, \beta)$  ( $\alpha < \beta$ ), we add  $N(N-1)/2$  new vertices  $(\alpha, \beta)$  (colored in blue) corresponding to the type-(ii) basis states in (C1). Last, we add  $N$  new vertices  $(\alpha, \alpha)$  ( $\alpha = 1, \dots, N$ ) and connect them to the vertices  $\alpha$ . Obviously, all the vertices are connected, which immediately means that any given basis state of the form (C1) can be transferred to an arbitrary state by the action of the Hamiltonian except when  $\mathcal{N}_c = 1, L_0$ .

The two exceptional cases  $\mathcal{N}_c = 1$  and  $L_0$  can be handled without relying on the induction. In fact, in the above two cases we use strings of (projected) hopping operators to realize  $\text{SU}(N)$  “spin-flips” on a pair of distant sites that allow us to transform any given state to an arbitrary one. Therefore, we see that the effective Hamiltonian (33) is irreducible in the  $(L_0 + 1)$ -site system as well, which completes the proof.

### Appendix D: Supersymmetry $\text{SU}(N|1)$

In Eq. (41), we have seen that the fermion operators (40) projected onto the subspace spanned by the Kondo singlet  $|\bullet\rangle_i$  and the fully-occupied state  $|N; \alpha\rangle_i$  do not obey the standard anti-commutation relations. In fact, they satisfy the anti-commutation relations of the fermionic generators of the super Lie algebra  $\text{SU}(N|1)$  (for a quick introduction to  $\text{SU}(N|1)$ , see appendix A of Ref. [82]).

#### 1. Definition

The superalgebra  $\text{SU}(N|1)$  consists of  $N^2$  bosonic and  $2N$  fermionic generators. The bosonic generators are given by the



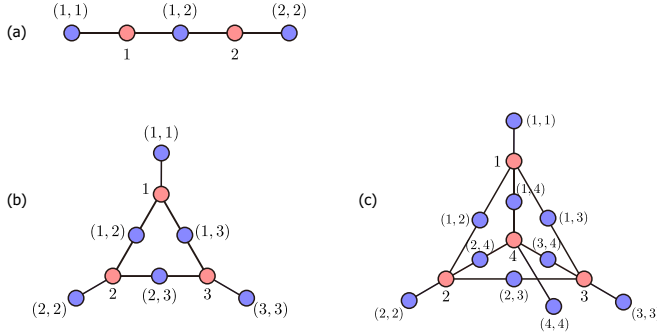


FIG. 13. Graphical representation of the connectivity introduced by the hopping between  $L_0$  and  $(L_0 + 1)$  for (a)  $N = 2$ , (b)  $N = 3$ , and (c)  $N = 4$ . The  $N(N + 3)/2$  groups of the basis states in (C1) are represented by the vertices (both red and blue). By the assumption, all the states *within* each group are connected to each other by the  $L_0$ -site Hamiltonian. The hopping between the sites  $L_0$  and  $L_0 + 1$  introduces the edges connecting these vertices (see the text for how these graphs are drawn).

following  $(N + 1) \times (N + 1)$  block-diagonal matrices:

$$\mathcal{S}^A = \begin{pmatrix} G^A & 0 \\ 0 & 0 \end{pmatrix} \quad (A = 1, \dots, N^2 - 1), \quad \mathcal{K} = \begin{pmatrix} \mathbf{1}_N & 0 \\ 0 & N \end{pmatrix} \quad (\text{D1})$$

with  $G^A$  being the  $\text{SU}(N)$  generators in the defining representations  $N$  which are normalized as:

$$\text{Tr}(G^A G^B) = \delta^{AB}.$$

On top of the above  $N^2$  bosonic generators, there are  $2N$  fermionic ones:

$$\mathcal{Q}_\alpha := \begin{pmatrix} \mathbf{0}_N & \boldsymbol{\tau}_\alpha \\ \mathbf{0}_{1 \times N} & 0 \end{pmatrix}, \quad \tilde{\mathcal{Q}}_\alpha := \begin{pmatrix} \mathbf{0}_N & \mathbf{0}_{N \times 1} \\ (\boldsymbol{\tau}_\alpha)^T & 0 \end{pmatrix} \quad (\alpha = 1, \dots, N), \quad (\text{D2})$$

where the  $N$ -component column vector  $\boldsymbol{\tau}_{\alpha 1}$  has only one non-zero entry:

$$\boldsymbol{\tau}_\alpha = (0, \dots, 0, 1, 0, \dots, 0)^T \quad (\text{D3})$$

and hence  $\tilde{\mathcal{Q}}_\alpha = (\mathcal{Q}_\alpha)^T$  holds. Physically, the fermionic generators bring about transitions between the first  $N \times N$  block and the second one-dimensional one.

The above generators satisfy the following algebra:

$$[\mathcal{S}^A, \mathcal{S}^B] = i f^{ABC} \mathcal{S}^C, \quad [\mathcal{K}, \mathcal{S}^A] = 0 \quad (\text{D4a})$$

$$\{\mathcal{Q}_\alpha, \mathcal{Q}_\beta\} = \{\tilde{\mathcal{Q}}_\alpha, \tilde{\mathcal{Q}}_\beta\} = 0 \quad (\text{D4b})$$

$$\{\mathcal{Q}_\alpha, \tilde{\mathcal{Q}}_\beta\} = [G^A]_{\beta\alpha} \mathcal{S}^A + \frac{1}{N} \delta_{\alpha\beta} \mathcal{K} \quad (\text{D4c})$$

$$[\mathcal{S}^A, \mathcal{Q}_\alpha] = \mathcal{Q}_\beta [S^A]_{\beta\alpha}, \quad [\mathcal{S}^A, \tilde{\mathcal{Q}}_\alpha] = -\tilde{\mathcal{Q}}_\beta [S^A]_{\alpha\beta} = \tilde{\mathcal{Q}}_\beta [-(S^A)^T]_{\beta\alpha} \quad (\text{D4c})$$

$$[\mathcal{K}, \mathcal{Q}_\alpha] = -(N - 1) \mathcal{Q}_\alpha, \quad [\mathcal{K}, \tilde{\mathcal{Q}}_\alpha] = (N - 1) \tilde{\mathcal{Q}}_\alpha. \quad (\text{D4d})$$

It is helpful to write down the right-hand side of (D4b) explicitly in the matrix form:

$$[G^A]_{\beta\alpha} \mathcal{S}^A + \frac{1}{N} \delta_{\alpha\beta} \mathcal{K} = \begin{pmatrix} \mathbf{e}_{\alpha\beta} & 0 \\ 0 & \delta_{\alpha\beta} \end{pmatrix}, \quad (\text{D5})$$

where the  $N \times N$  matrices  $\mathbf{e}_{\alpha\beta}$  ( $\alpha, \beta = 1, \dots, N$ ) are defined by  $[\mathbf{e}_{\alpha\beta}]_{ij} = \delta_{i\alpha} \delta_{j\beta}$ . Out of the above  $N(N + 2)$  generators, we can construct the quadratic Casimir as:

$$\mathcal{C}_2 = \sum_{A=1}^{N^2-1} \mathcal{S}^A \mathcal{S}^A - \frac{1}{N(N-1)} \mathcal{K}^2 - \sum_{\alpha=1}^N (\mathcal{Q}_\alpha \tilde{\mathcal{Q}}_\alpha - \tilde{\mathcal{Q}}_\alpha \mathcal{Q}_\alpha). \quad (\text{D6})$$

## 2. Fock representations

### a. Abrikosov construction (slave boson)

There are two different ways to realize the  $\text{SU}(N|1)$  algebra (D4a)-(D4d) in terms of bosons and fermions. One is to use  $N$  species of (ordinary) fermions  $\{f_\alpha^\dagger\}$  and one species of boson  $b$  (construction “F-B”) which is known as the *slave-boson representation* [74]:

$$\hat{\mathcal{S}}^A = f_\alpha^\dagger [S_A]_{\alpha\beta} f_\beta, \quad \hat{\mathcal{K}} = n_F + N n_B \quad (\text{D7a})$$

$$\hat{\mathcal{Q}}_\alpha = f_\alpha^\dagger b, \quad \hat{\tilde{\mathcal{Q}}}_\alpha = b^\dagger f_\alpha \quad (\alpha = 1, \dots, N), \quad (\text{D7b})$$

where the fermion and boson numbers are defined by  $n_F = \sum_\alpha f_\alpha^\dagger f_\alpha$  and  $n_B = b^\dagger b$ , respectively. Obviously,  $n := n_F + n_B$  is conserved and can be used to label irreducible representations of  $\text{SU}(N|1)$ . In fact, the quadratic Casimir in (D6) is given by:

$$\mathcal{C}_2^{\text{F-B}}(n) = \frac{N}{N-1} n \{(N-1) - n\}. \quad (\text{D8})$$

We can easily check that the choice  $n = 1$  correctly reproduces the expressions (D1) and (D2). For general  $n$ , the representation consists of  $\min(N, n) + 1$  different irreducible representations of  $\text{SU}(N)$

$$\bigoplus_{n_F=0}^{\min(N,n)} \left[ \begin{array}{c} \boxed{n_B = n - n_F} \end{array} \right] \quad (\text{D9})$$

corresponding to the possible fermion numbers  $n_F [= 0, \dots, \min(N, n)]$ .

### b. Schwinger construction (slave fermion)

Another construction uses  $N$  species of bosons  $b_\alpha^\dagger$  and one fermion  $f^\dagger$  (construction “B-F”; *slave-fermion representation*):

$$\hat{\mathcal{S}}^A = b_\alpha^\dagger [S_A]_{\alpha\beta} b_\beta, \quad \hat{\mathcal{K}} = n_B + N n_F \quad (\text{D10a})$$

$$\hat{\mathcal{Q}}_\alpha = b_\alpha^\dagger f, \quad \hat{\tilde{\mathcal{Q}}}_\alpha = f^\dagger b_\alpha \quad (\alpha = 1, \dots, N). \quad (\text{D10b})$$

The boson and fermion numbers are defined by  $n_B = \sum_{\alpha} b_{\alpha}^{\dagger} b_{\alpha}$  and  $n_F = f^{\dagger} f$ , respectively, and the quadratic Casimir  $C_2$  now is determined by  $n = n_F + n_B$  as:

$$C_2^{B-F}(n) = \frac{N-2}{N-1} n \{(N-1) + n\} . \quad (D11)$$

Since the fermion number can take only two values  $n_F = 0, 1$ , the representation specified by  $n$  is made of two  $SU(N)$  irreducible representations:

$$\left[ \underbrace{\square \square \square \square}_{n} (n_F = 0) \right] \oplus \left[ \underbrace{\square \square \square \square}_{n-1} (n_F = 1) \right] . \quad (D12)$$

Although the conserved  $n = n_F + n_B$  again plays a crucial role in specifying the irreducible representations, the repre-

sentations (D7a)-(D7b) and (D10a)-(D10b) in general realize *different* irreducible representations even for the same  $n$  (except for  $n = 1$ ).

The  $n = 2$  representation used in Sec. VC is constructed as follows. First, the  $N(N+3)/2$  basis states are given by:

$$(n_B, n_F) = (2, 0) : \dots \square \square$$

$$|(\alpha, \alpha)\rangle = \frac{1}{\sqrt{2}} (b_{\alpha}^{\dagger})^2 |0\rangle \quad (D13a)$$

$$|(\alpha, \beta)\rangle = b_{\alpha}^{\dagger} b_{\beta}^{\dagger} |0\rangle \quad (\alpha < \beta) .$$

$$(n_B, n_F) = (1, 1) : \dots \square$$

$$|N; \alpha\rangle = b_{\alpha}^{\dagger} f^{\dagger} |0\rangle \quad (\alpha = 1, \dots, N) . \quad (D13b)$$

We can find all the matrix elements of the generators by applying the expressions (D10a)–(D10b) to the above basis states.

- 
- [1] Y. Q. Li, M. Ma, D. N. Shi, and F. C. Zhang, *Physical Review Letters* **81**, 3527 (1998).
- [2] F. Wu, I. Sodemann, Y. Araki, A. H. MacDonald, and T. Jolicoeur, *Phys. Rev. B* **90**, 235432 (2014).
- [3] M. A. Cazalilla, A. F. Ho, and M. Ueda, *New J. Phys.* **11**, 103033 (2009).
- [4] A. V. Gorshkov, M. Hermele, V. Gurarie, C. Xu, P. S. Julienne, J. Ye, P. Zoller, E. Demler, M. D. Lukin, and A. M. Rey, *Nat Phys* **6**, 289 (2010).
- [5] M. A. Cazalilla and A. M. Rey, *Rep. Prog. Phys.* **77**, 124401 (2014).
- [6] S. Capponi, P. Lecheminant, and K. Totsuka, *Ann. Phys.* **367**, 50 (2016).
- [7] S. Taie, R. Yamazaki, S. Sugawa, and Y. Takahashi, *Nat Phys* **8**, 825 (2012).
- [8] C. Hofrichter, L. Riegger, F. Scazza, M. Höfer, D. R. Fernandes, I. Bloch, and S. Fölling, *Phys. Rev. X* **6**, 021030 (2016).
- [9] H. Ozawa, S. Taie, Y. Takasu, and Y. Takahashi, *Phys. Rev. Lett.* **121**, 225303 (2018).
- [10] S. Taie, E. Ibarra-García-Padilla, N. Nishizawa, Y. Takasu, Y. Kuno, H.-T. Wei, R. T. Scalettar, K. R. A. Hazzard, and Y. Takahashi, *Nat. Phys.* **18**, 1356 (2022).
- [11] M. Hermele and V. Gurarie, *Phys. Rev. B* **84**, 174441 (2011).
- [12] P. Corboz, M. Lajkó, A. M. Läuchli, K. Penc, and F. Mila, *Phys. Rev. X* **2**, 041013 (2012).
- [13] J.-Y. Chen, J.-W. Li, P. Nataf, S. Capponi, M. Mambrini, K. Totsuka, H.-H. Tu, A. Weichselbaum, J. von Delft, and D. Poilblanc, *Phys. Rev. B* **104**, 235104 (2021).
- [14] C. Honerkamp and W. Hofstetter, *Phys. Rev. Lett.* **92**, 170403 (2004).
- [15] R. W. Cherng, G. Refael, and E. Demler, *Phys. Rev. Lett.* **99**, 130406 (2007).
- [16] P. Lecheminant, E. Boulat, and P. Azaria, *Phys. Rev. Lett.* **95**, 240402 (2005).
- [17] A. Rapp, G. Zaránd, C. Honerkamp, and W. Hofstetter, *Phys. Rev. Lett.* **98**, 160405 (2007).
- [18] S. Capponi, G. Roux, P. Lecheminant, P. Azaria, E. Boulat, and S. R. White, *Phys. Rev. A* **77**, 013624 (2008).
- [19] H. Yoshida and H. Katsura, *Phys. Rev. B* **105**, 024520 (2022).
- [20] H. Katsura and A. Tanaka, *Phys. Rev. A* **87**, 013617 (2013).
- [21] S.-K. Yip, B.-L. Huang, and J.-S. Kao, *Phys. Rev. A* **89**, 043610 (2014).
- [22] Y. Li, E. H. Lieb, and C. Wu, *Phys. Rev. Lett.* **112**, 217201 (2014).
- [23] E. Bobrow, K. Stubis, and Y. Li, *Phys. Rev. B* **98**, 180101 (2018).
- [24] K. Tamura and H. Katsura, *J. Stat. Phys.* **182**, 16 (2021).
- [25] M. Foss-Feig, M. Hermele, and A. M. Rey, *Phys. Rev. A* **81**, 051603 (2010).
- [26] M. Nakagawa and N. Kawakami, *Phys. Rev. Lett.* **115**, 165303 (2015).
- [27] L. Isaev and A. M. Rey, *Phys. Rev. Lett.* **115**, 165302 (2015).
- [28] L. Riegger, N. Darkwah Oppong, M. Höfer, D. R. Fernandes, I. Bloch, and S. Fölling, *Phys. Rev. Lett.* **120**, 143601 (2018).
- [29] K. Ono, Y. Amano, T. Higomoto, Y. Saito, and Y. Takahashi, *Phys. Rev. A* **103**, L041303 (2021).
- [30] C. Zener, *Phys. Rev.* **82**, 403 (1951).
- [31] P. W. Anderson and H. Hasegawa, *Phys. Rev.* **100**, 675 (1955).
- [32] P. G. de Gennes, *Phys. Rev.* **118**, 141 (1960).
- [33] K. Kubo, *J. Phys. Soc. Jpn.* **51**, 782 (1982).
- [34] S. Yunoki, J. Hu, A. L. Malvezzi, A. Moreo, N. Furukawa, and E. Dagotto, *Phys. Rev. Lett.* **80**, 845 (1998).
- [35] E. Dagotto, S. Yunoki, A. L. Malvezzi, A. Moreo, J. Hu, S. Capponi, D. Poilblanc, and N. Furukawa, *Phys. Rev. B* **58**, 6414 (1998).
- [36] M. Sgrist, H. Tsunetsugu, K. Ueda, and T. M. Rice, *Phys. Rev. B* **46**, 13838 (1992).
- [37] M. Troyer and D. Würtz, *Phys. Rev. B* **47**, 2886 (1993).
- [38] I. P. McCulloch, A. Juozapavicius, A. Rosengren, and M. Gulácsi, *Phys. Rev. B* **65**, 052410 (2002).
- [39] R. Peters and N. Kawakami, *Phys. Rev. B* **86**, 165107 (2012).
- [40] H. Tsunetsugu, M. Sgrist, and K. Ueda, *Rev. Mod. Phys.* **69**, 809 (1997).
- [41] M. Gulácsi, *Adv. Phys.* **53**, 769 (2004).
- [42] P. Coleman, *Introduction to Many-Body Physics* (Cambridge University Press, 2015).
- [43] To realize the situation  $n_e = 1$ , strong enough  $U^{(e)}$  is necessary. As  $t^{(e)}$  is negligibly small, we can easily find the condition for  $U^{(e)}$  with the effects of the harmonic trap (the trap frequency  $\omega_{\text{trap}}$ ) taken into account:  $U^{(e)} > (1/8) \mathcal{N}_e^2 m \omega_{\text{trap}}^2 a_0^2$  ( $a_0$  is the lattice constant and  $\mathcal{N}_e$  denotes the number of the  $e$  fermions). This condition is fulfilled in the usual experimental settings.
- [44] H. Georgi, *Lie Algebras in Particle Physics* (Perseus Books,

- 1999).
- [45] In typical experimental settings,  $\tilde{V}_H^{g-e} > 0$  for all  $N$  and alkaline-earth fermions. Due to positive  $U^{(e)}$  and  $\tilde{V}_H^{g-e}$ , states with  $e$ -fermions uniformly occupying the lattice  $n_{e,i} = 1$  are favored.
- [46] P. Coleman, *Phys. Rev. B* **28**, 5255 (1983).
- [47] N. Read, D. M. Newns, and S. Doniach, *Phys. Rev. B* **30**, 3841 (1984).
- [48] M. Raczkowski and F. F. Assaad, *Phys. Rev. Research* **2**, 013276 (2020).
- [49] P. Sinjukow and W. Nolting, *Phys. Rev. B* **65**, 212303 (2002).
- [50] X. Zhang, M. Bishof, S. L. Bromley, C. V. Kraus, M. S. Safronova, P. Zoller, A. M. Rey, and J. Ye, *Science* **345**, 1467 (2014).
- [51] G. Cappellini, M. Mancini, G. Pagano, P. Lombardi, L. Livi, M. Siciliani de Cumis, P. Cancio, M. Pizzocaro, D. Calonico, F. Levi, C. Sias, J. Catani, M. Inguscio, and L. Fallani, *Phys. Rev. Lett.* **113**, 120402 (2014).
- [52] F. Scazza, C. Hofrichter, M. Höfer, P. C. De Groot, I. Bloch, and S. Fölling, *Nat. Phys.* **10**, 779 (2014).
- [53] K. Ono, J. Kobayashi, Y. Amano, K. Sato, and Y. Takahashi, *Phys. Rev. A* **99**, 032707 (2019).
- [54] When  $N = 2$ , we can apply a unitary transformation  $i\sigma^y$  to  $(c_\uparrow, c_\downarrow)^T$  to make  $\hat{s} \rightarrow \hat{s}$ .
- [55] P. Lecheminant, *Nucl. Phys. B* **901**, 510 (2015).
- [56] K. Wamer, M. Lajko, F. Mila, and I. Affleck, *Nucl. Phys. B* **952**, 114932 (2020).
- [57] P. Nataf, S. Gozel, and F. Mila, *Phys. Rev. B* **104**, L180411 (2021).
- [58] K. Duivenvoorden and T. Quella, *Phys. Rev. B* **87**, 125145 (2013).
- [59] A. M. Tsvelik, *Phys. Rev. Lett.* **72**, 1048 (1994).
- [60] In fact, the state space of an  $N$ -component fermion is isomorphic to  $\mathbb{C}P^{N-1}$ .
- [61] In periodic systems, the matrix elements for the hopping *across* the boundary acquire an additional fermion sign  $(-1)^{\mathcal{N}_c-1}$  ( $\mathcal{N}_c$  is the total fermion number in the system). Due to this factor, the condition for positivity depends explicitly on the parity of the fermion number.
- [62] H. Tasaki, *Physics and Mathematics of Quantum Many-Body Systems* (Springer, 2020).
- [63] When the periodic boundary condition is imposed, on the other hand, cyclic permutation of the spin configurations is allowed [64]. However, it is clear that cyclic permutations do not connect all the allowed states which still prevents the application of the Perron-Frobenius theorem. In fact, for finite periodic systems, states other than ferromagnetic ones can have lower energies.
- [64] W. J. Caspers and P. L. Iske, *Physica A*: **157**, 1033 (1989).
- [65] M. Ogata and H. Shiba, *Phys. Rev. B* **41**, 2326 (1990).
- [66] C. Lacroix, *Solid State Commun.* **54**, 991 (1985).
- [67] V. Bois, S. Capponi, P. Lecheminant, M. Moliner, and K. Totsuka, *Phys. Rev. B* **91**, 075121 (2015).
- [68] When  $J_K$  is antiferromagnetic, the condition of the minimal Kondo coupling  $\mathbf{z}_{c,i}^* \cdot \mathbf{z}(\mathbf{q}_i) = 0$  does not favor a particular direction of the fermion state  $\mathbf{z}_{c,i}^*$  and the following argument fails.
- [69] P. Schlottmann, *Phys. Rev. Lett.* **69**, 2396 (1992).
- [70] N. Kawakami, *Phys. Rev. B* **47**, 2928 (1993).
- [71] P. Schlottmann, *J. Phys. Condens. Matter* **5**, 313 (1993).
- [72] P. B. Wiegmann, *Phys. Rev. Lett.* **60**, 821 (1988).
- [73] P. A. Bares and G. Blatter, *Phys. Rev. Lett.* **64**, 2567 (1990).
- [74] P. Coleman, *Phys. Rev. B* **29**, 3035 (1984).
- [75] If we normalize the  $SU(N)$  generators as  $\text{Tr}(S^A S^B) = \delta^{AB}/2$ , the condition reads as:  $\mathcal{J} = 2t$  which is well-known in the  $SU(2)$  literature.
- [76] A. E. Sikkema, I. Affleck, and S. R. White, *Phys. Rev. Lett.* **79**, 929 (1997).
- [77] R. Masui and K. Totsuka, *Phys. Rev. B* **106**, 014411 (2022).
- [78] D. P. Arovas, K. Hasebe, X.-L. Qi, and S.-C. Zhang, *Phys. Rev. B* **79**, 224404 (2009).
- [79] K. Hasebe and K. Totsuka, *Phys. Rev. B* **84**, 104426 (2011).
- [80] K. Hasebe and K. Totsuka, *Phys. Rev. B* **87**, 045115 (2013).
- [81] When  $\mathcal{N}_c = 1$ ,  $\mathbf{B}_{(\alpha,\beta)}$  are not irreducible, while when  $\mathcal{N}_c = L_0$ ,  $\mathbf{B}_\alpha$  is not. Therefore, these two cases must be treated separately.
- [82] K. Hasebe, *Nucl. Phys. B* **853**, 777 (2011).